THESIS ABSTRACT

THE OHIO STATE UNIVERSITY
GRADUATE SCHOOL

NAME: Kotsas, Panagiotis **QUARTER/YEAR:** Spring 96

DEPARTMENT: Biomedical Engineering **DEGREE:** Master of Science

ADVISER'S NAME: Cornhill, John, Fredrick

TITLE OF THESIS: A new automated method for three-dimensional registration of MR images of the head.

A new technique for three-dimensional image registration was developed and tested using T1- and T2-weighted Magnetic Resonance image studies of the head. The method uses the fuzzy c-means classification algorithm for outlining the surface contours and then minimizes iteratively the mean squared value of the voxel per voxel weighted ratio of the two trilinearly interpolated cubic voxel volumes. A total of 200 two-dimensional and 240 three-dimensional registration experiments were performed and showed that the method is surface based, it has registration accuracy better than one degree for rotations and one voxel for translations and it is not affected by the deterioration in the imaging resolution for voxel sizes up to 1.8 mm.

_____

Adviser's Signature

A NEW AUTOMATED METHOD FOR THREE-DIMENSIONAL REGISTRATION OF MR IMAGES OF THE HEAD

A Thesis

Presented in Partial Fulfillment of the Requirements for

the degree Master of Science in the

Graduate School of The Ohio State University

by

Panagiotis Kotsas, B.Sc.

* * * * *

The Ohio State University

1996

Master's Examination Committee:

J. Fredrick Cornhill, D.Phil.

David W. Piraino, M.D.

Approved by:

_____

Adviser
Department of Biomedical Engineering

To my parents Dimitris and Vassiliki

for all the sacrifices they have been making for me

ACKNOWLEDGEMENTS

I want to express my gratitude to Dr. David W. Piraino whose enthousiastic guidance, innovative spirit, and engineering insight, inspired me throughout the course of this work. My appreciation goes also to Dr. J.Fredrick Cornhill for his very useful suggestions and comments. I also want to thank Ms. Christine Kabrera whose comments improved dramatically this document. Very important was the help that I received during the data collection procedures from Mr. Vassilis Gougoulidis and Mr. Dominik Meyer, I am thankful to them. The conversion of the ACR-NEMA 2.0 imaging format was made possible due to the use of the STACR utility, programmed and provided to me by Dr. Rim Cothren from the Department of Biomedical Engineering of the Cleveland Clinic Foundation, I am grateful to him. I would also like to express my gratitude to all the members of the Graduate Studies Committee of the Department of Biomedical Engineering of the Ohio State University for giving me the opportunity to study in the United States. Finally, my most sincere gratitude goes to my parents and my sister Popi for encouraging me and helping me not to quit and to Vangelio, my girlfriend, for her warm and encouraging attitude.

VITA

November 4, 1969.....Born - Kavala, Greece

1993.....B.S. in Electrical Engineering,
Aristotelian University of
Thessaloniki, Greece

1993-Present.....Graduate Research Associate,
The Ohio State University,
Columbus, Ohio, USA

PUBLICATIONS

[1] Kotsas P, Piraino D, Recht M, Richmond B. Comparison of an adaptive wavelet based and a DCT based algorithm for image compression. 80th Scientific Assembly and Annual Meeting of Radiological Society of North America, Scientific Session, December 1994, Chicago, Illinois.

[2] Kotsas P, Piraino D, Recht M, Richmond B. Comparison of an adaptive wavelet based and a DCT based algorithm for image compression. 80th Scientific Assembly and Annual Meeting of Radiological Society of North America, Scientific Exhibits, December 1994, Chicago, Illinois.

[3] Kotsas P, Recht M, Richmond B, Schills J, Piraino D. New automated method for registration of bone anatomy and quantitative evaluation of changes in alignment in radiographs. Symposium for Computer Assisted Radiology, June 1994, Winston-Salem, North Carolina.

[4] Piraino D, Kotsas P, Recht M, Richmond M. Automated method for 3D registration of MR images. 80th Scientific Assembly and Annual Meeting of Radiological Society of North America, Scientific Session, December 1994, Chicago, Illinois.

[5] Piraino D, Kotsas P. Artificial neural network registration of simulated 3D images. IEEE International Conference on Neural Networks, Conference Proceedings, Vol. 6, pp4017-4021, July 1994, Orlando, Florida.

[6] Kotsas P, Pappas K, Strintzis M, Maglaveras N. Non-stationary ECG signal analysis using the Wigner-Ville transform and wavelets. IEEE Computers I n Cardiology, Conference Proceedings, pp499-502, September 1993, London, United Kingdom.

FIELDS OF STUDY

Major Field: Biomedical Engineering

LIST OF TABLES

TABLE PAGE

LIST OF FIGURES

FIGURE PAGE

TABLE OF CONTENTS

CHAPTER I

INTRODUCTION

1.1 Medical image registration

Medical imaging modalities (Computed Tomography, Magnetic Resonance, Positron Emission Tomography, Single Photon Emission Computed Tomography) provide information that illustrates human brain anatomy and function. This information is often complementary and its correlative use can improve diagnostic accuracy. For example, the merging of fine anatomic detail from MR images of the brain with functional PET images allows the measurement of regional cerebral function[20]. Likewise, MR and CT images describe complementary morphologic features. Bone calcifications are seen best on CT images, while soft tissue structures are differentiated better by MR[17].

Medical image registration is the procedure of geometrically aligning two image volumes so that voxels representing the same anatomical structure may be superimposed one on another[14]. Registration techniques make it possible to superimpose features from one image study over those of another image study from a different modality. These techniques can also be applied to studies of

the same modality taken at different times so that point-by-point arithmetic operations such as image averaging, subtraction and correlation can be performed[4].

In recent years there has been a rapid growth of neurological applications of medical

image registration with applications that address both diagnosis and therapy. Registration is progressively playing a larger role in image interpretation in many different procedures. According to Evans et al.[19], image registration has found use in the areas of:

1) disease diagnosis

2) longitudinal monitoring of disease progress or remission

3) preoperative evaluation and neurosurgical planning

4) image guided neurosurgery

5) radiotherapy and radiosurgery treatment planning

6) functional neuroanatomy of sensorimotor and cognitive processes

7) morphometric analysis of neuroanatomic variability.

Several methods for medical image registration have been proposed. There are device-based methods and feature-based methods. The device-based methods use head-holding devices that keep the patient's head at a fixed orientation and/or external fiducial markers visible in both image sets. The fiducial marker coordinates are used to estimate the geometric transformation that establishes a one-to-one mapping between the two image spaces. These methods are non-automated, technically demanding and require a significant amount of effort at the time of each scan[5,21]. Furthermore they have been found to be less accurate than feature-based techniques. Strother et al.[14]

compared the accuracy of a fiducial marker system with the accuracy of feature-based techniques and reported that "it is not possible to fix the head accurately enough relative to external fiducial markers to obtain registration results as good as those obtained by non-fiducial techniques."

Feature-based methods use the anatomic information inherent in the two image sets. These techniques follow a general methodology with four steps[12]:

a) extraction of features in each image

b) pairing of these features

c) choice of geometric transformation and estimation of its parameters

d) application of this transformation.

Feature-based techniques do not require any special procedures or devices at imaging time and may be applied retrospectively[5,21]. The extraction of the anatomic features can be performed either manually with the assistance of an expert user[13] or automatically. For example, in the interactive method developed by Kapouleas et al.[13], the user is asked to specify the interhemispheric fissure plane in three dimensions for both image volumes by specifying its endpoints in every axial MR section. The planes are then used to align the image volumes. The disadvantages of this method are that it requires a large amount of time from the user (1 hour per registration case) and also that the registration accuracy is affected by the user's performance.

Three different types of automated feature-based techniques can be defined when they are classified according to the type of the anatomic features they use[18]. Correlation methods make use of the voxel intensity distributions; the principal axes method makes use of the spatial moments of the three-dimensional volumes or surfaces;

and the surface fitting method uses the anatomic surfaces in the two image volumes. Automated registration methods can also be categorized according to their ability to perform cross-modality image registration. Correlation methods are not able to register image studies from different modalities because the signal intensity distributions differ. Principal axes and surface fitting methods use the shape characteristics of the two image volumes that are not affected by the difference in signal intensity distributions and therefore these two methods are able to perform cross-modality registration.

Another classification criterion is the dimensionality of the registration problem. Two-dimensional registration methods assume only in-plane displacements and adjust for one rotational and two translational parameters, whereas three-dimensional methods adjust for three rotational and three translational parameters. For example, in the case of digital subtraction angiography, a major problem concerns the movements of the patient, which diminish the benefit of the subtraction procedure[15]. X-ray images capture in-plane motion and therefore the registration problem is two-dimensional. On the other hand, the motion of the patient's head inside the MR imaging machine is captured by the three-dimensional imaging system and therefore the registration algorithms that deal with MR data are three-dimensional.

The way that the geometric transformation parameters are estimated can also be used to discriminate registration methods. The principal axes method gives a closed form solution to the registration problem, whereas the correlation and surface fitting methods solve the problem iteratively.

The rest of this chapter will provide an overview of the main existing automated, feature-based registration techniques. The principles, the accuracy and the literature

applications of the correlation, surface fitting and principal axes methods will be presented.

1.2 Correlation methods

Correlation methods register medical images by maximizing a similarity or minimizing a disparity criterion between the images. The similarity or disparity criterion used is signal intensity based, and it is maximized or minimized iteratively. Correlation methods are limited in their application because they require that the images be from the same modality. Some of the criteria proposed[15,16] require that the signal intensity distributions be exactly the same. When this does not happen, signal intensity scaling is considered as an additional parameter to be adjusted within the iteration loop. A correlation criterion that was applied by Woods et al.[9,10] for MR-PET image registration is the ratio image uniformity criterion. This application involves a preprocessing step during which the images are segmented to create the same types of anatomic regions and therefore the same signal intensity distributions. Various criteria have been proposed in the literature. The most important ones are:

a) Cross-correlation coefficient [8]

b) Stochastic sign change [15,16]

c) Maximum region overlap [11,12]

d) Ratio image uniformity [9,10]

1.2.1 Cross-correlation coefficient

The cross-correlation coefficient for two images A and B is given by the formula[8]:

$$r = \frac{\sum_i (A_i - \overline{A})(B_i - \overline{B})}{\sqrt{\sum_i (A_i - \overline{A})^2 \sum_i (B_i - \overline{B})^2}} \qquad (1.1)$$

where i is an index to the image voxels and $\overline{A}, \overline{B}$ are the mean intensity values of the images over the whole voxel area. Junck et al.[8] use this coefficient for two-dimensional alignment of PET scans. They show that the maximum location of the cross-correlation coefficient is the same as the maximum location of the cross-product coefficient $\sum_i A_i B_i$. Therefore they maximize the criterion by computing the cross-product value for the whole range of the geometric transformation parameters using steps of $\Delta\vartheta = 1$degree for rotations and $\Delta\chi = \Delta y = 1$voxel for translations. To achieve better accuracy, they fit a quadratic function in $\Delta\chi$,Δy and $\Delta\vartheta$ to the cross-product data and find its peak. The peak position is recalculated after each translational and rotational correction of one image relative to another. The accuracy of the method is defined as the standard deviations of the transformation parameters among five different levels of the patient's head: 0.54 mm for x and y translations and 0.8 degrees for xy plane rotation[8].

1.2.2 Stochastic Sign Change

The stochastic sign change criterion proposed by Venot et al.[15] is defined as "the number of sign changes in the sequence of the values of the difference image." In order to understand the rationale of the use of this similarity measure, consider two images

A(i,j) and B(i,j) of the same object and the same modality that are registered to each other. If we assume that the signal intensity distributions are identical, then the difference image D(i,j)=A(i,j)-B(i,j) will take values equal to the noise measurement differences. If we also consider the noise as additive, zero mean with a symmetric density function, then we find that the difference image values are either positive or negative and there are many sign changes in the sequence of D(i,j) because there is an equal probability of 0.5 for each sign + or -. When the two images are not registered, the difference image takes values equal to the differences of the signal intensity distributions. These differences are greater than the noise measurement differences, and therefore the sign changes number reduces. The maximization of the number of sign changes can be performed iteratively using the Simplex optimization technique[16,24].

It is obvious that the method may fail when the signal intensity distributions are not strictly identical. Gerlot-Chiron and Bizais[11,12] reported that "computing the number of sign changes in the difference image corresponds to computing the number of registered pixels only if the expected difference is zero for these pixels." Venot et al.[15] and Herbin et al.[16] solved this problem by using intensity scaling as an additional parameter to be adjusted by the method.

The Sign Change criterion was applied by Venot et al.[15] for two-dimensional translational adjustment of X-ray digitized images for improving the quality of subtraction angiographic images. It was also applied by Herbin et al.[16] for rotational and translational adjustment of digitized video medical images. In both of these studies,

no quantitative measure of the accuracy of the method is given. Results are given only for a few example registration cases. In such a case of translational adjustment of x-ray images presented by Venot et al.[15], the Sign Change criterion was compared to the Correlation Coefficient criterion and was found to be more accurate.

1.2.3 Maximum Region Overlap

The Maximum Region Overlap criterion was introduced by Gerlot-Chiron and Bizais[11,12]. It aims at maximizing the overlap of the registrable areas in the two images. The method is based on the idea that the histogram of the difference image exhibits a low signal-intensity peak caused by the registered voxels in the two images. The shape of this peak is related to noise statistical properties. The area of this peak becomes maximum when the two images are registered. The algorithm aims at maximizing the peak area of the histogram, which is computed for all the possible values of the geometric transformation parameters using a matched filter:

$$RO(p)=\sum_{i=-n}^{n} a(i)\, h(i+p) \qquad (1.2)$$

where a(i) is a Gaussian matched filter impulse response $G(0,\sigma)$, h is the histogram distribution of intensity in the difference image and p is the location of the peak of the registered voxels area of the histogram. The filter was chosen to be Gaussian because noise can be considered Gaussian in most medical imaging applications[11,12].

According to Gerlot-Chiron and Bizais[11], the method can be considered as a generalization of the Sign Change criterion for the case that the signal-intensity distributions in the two images are not identical. The method was used for two-

dimensional translational adjustment of lung scintigrams. In order to test the performance of the method, white and colored noise was added to the images. The error was estimated as the difference of the applied geometric transformation from the estimated one. The errors were zero for both cases of white and colored additive noise.

1.2.4 Ratio image uniformity

The ratio image uniformity criterion was introduced by Woods et al.[9,10]. To align the two images, the algorithm calculates the ratio of one image to the other on a voxel-by-voxel basis and then iteratively minimizes the variance of this ratio. The method is based on the ideal assumption that in the case that the images are registered, the values of the voxels in one image, can result by multiplying the voxels in the other image with a constant multiplicative factor. When the images are not registered, the value of the multiplicative factor varies from voxel to voxel, creating a large variance of the ratio image values.

The method uses an iteration loop based on derivatives to minimize the variance of the ratio image, which is defined as the registration function. With each iteration, the first partial derivative of the registration function with respect to each of the transformation parameters is calculated. The parameter with the largest first partial derivative is adjusted. The second partial derivative with respect to the selected parameter is then used to estimate the value of the parameter at which the first partial derivative will be zero with the Newton-Raphson method[24]. This value is used in the next iteration. Convergence is reached when all of the first partial derivatives get values below a threshold value.

The ratio image uniformity method was applied by Woods et al.[9] for alignment of functional PET three dimensional images. As mentioned above, a modified version of the algorithm[10] was applied for MR-PET registration. The investigators used the post-registration distance of external fiducial markers as a measure of the positional errors resulting from the registration procedure. They reported that the positional errors are less than 1.745 mm for PET-PET registration and less than 3 mm for PET-MR registration. These results are verified by Strother et al.[14], who applied the method for MRI-MRI, PET-MRI and PET-PET registration. They reported positional errors at the range of 1 voxel.

1.3 Surface fitting method

Surface matching methods register images by using the anatomic surface models of the two images. The most important method in this category is the surface fitting method developed by Pelizzari et al.[7,18] at the University of Chicago. The method is referred to as the "head and hat" method because it fits a set of points ("hat") extracted from contours in one image to a surface model ("head") extracted from contours in the other image[7]. The surfaces are obtained by outlining contours on the slices of each image set, either manually[18] or by using a semiautomatic edge detection algorithm[5,6]. The head surface model is generated by the image that covers the larger area of the head or by the image with the higher resolution if the coverage of the head is comparable. The mean squared distance between the hat points and the head surface is minimized iteratively using a non-linear least-squares search technique introduced by Powell[24]. The distance is computed between the hat point and the intersection point of the head surface and the

line that connects the hat point with the centroid of the head surface. A linear interpolation step between the head surface contours is needed for the computation of the intersection point. The iteration loop adjusts for xy,yz,zx plane rotations, x,y,z axes translations and x,y,z axes linear scaling. The algorithm allows operator intervention to prealign the surfaces to prevent the search from converging to a local minimum. The problem of local minima is inherent in non-linear least-squares minimization techniques[24].

The method was applied by Pelizzari et al.[7] for registration of CT, MR, and PET images. It was also modified to perform registration of image space to physical space[18]. This application involves the use of a digitizer that is able to acquire a three dimensional model of the patient's skin surface. The skin surface model is then registered to the image generated surface. The surface fit method has been used also by several other groups[1,5,6,14] who tried to evaluate its accuracy. Based on these studies the following points are of interest:

a) For registration of MRI-PET images, the translational errors were found to be less than 2 mm in each direction and the rotational errors less than 2 degrees for each angle[5,6].

b) For registration of MR to patient surface, the positional error is in the range of 3-8 mm[18].

c) Missing data do not affect the accuracy of the method. For brain coverage as low as

40%, the registration position error remained less than 2mms in each direction[1].

d) The degree of initial misangulation does not affect the accuracy of the method[1].

e) The processing time is between 3 and 11 minutes, depending on the number of iterations[1].

1.4 Principal axes method

The principal axes transformation is known from the theory of rigid bodies. A rigid body may be located using the position of the center of its mass and the orientation of its principal axes with respect to its center of mass[2]. The principal axes are the axes of symmetry of the rigid body and form an orthogonal coordinate system with origin the center of mass of the rigid body. To register two images using the principal axes, the following steps are used[2]:

STEP 1: The two images are segmented and the object surfaces are defined using an automated[3] or manual[1] segmentation scheme. Two different implementations of the method exist. One uses the full volumes for the computation of the principal axes transformation and the other uses only the surface outlines.

STEP 2: The centers of mass of the two volumes or surfaces are computed for the two images to be registered using the formula:

$$[\bar{x},\bar{y},\bar{z}] = \text{Mean}[x,y,z] \qquad (1.3)$$

where x,y,z are the integer coordinates of an image voxel that belongs to the signal area or to the surface outline, the symbol Mean indicates the arithmetic mean over the set of

all voxels in each image volume or surface, and $\bar{x},\bar{y},\bar{z}$ denote the coordinates of the center of mass.

STEP 3: The centers of both volumes or surfaces are translated to the origin of the center of mass coordinate system using the translational adjustment formula:

$$[x',y',z'] = [x,y,z] - [\bar{x},\bar{y},\bar{z}] \tag{1.4}$$

STEP 4: The moments and products of inertia are computed as:

$$[I_{xx},I_{yy},I_{zz}] = \text{Mean}[x'^2,y'^2,z'^2] \tag{1.5}$$

$$[I_{xy},I_{xz},I_{yz}] = \text{Mean}[x'y',x'z',y'z'] \tag{1.6}$$

and the inertia matrix for each of the volumes or surfaces is formed as:

$$\mathbf{I} = \begin{bmatrix} I_{xx} & I_{xy} & I_{xz} \\ I_{yx} & I_{yy} & I_{yz} \\ I_{zx} & I_{zy} & I_{zz} \end{bmatrix} \tag{1.7}$$

with $I_{xy} = I_{yx}$, $I_{yz} = I_{zy}$, $I_{xz} = I_{zx}$.

STEP 5: The inertia matrices $\mathbf{I}_{1,2}$ for the two volumes or surfaces are expressed as a similarity transformation:

$$\mathbf{I}_i = \mathbf{S}_i \, \boldsymbol{I} \, \mathbf{S}_i^{\,T} \quad \text{with i = 1,2} \tag{1.8}$$

where $\boldsymbol{I}$ represents the inertia matrix as it is computed in the principal axes coordinate system and the rotation matrix $\mathbf{S}_i$ is the matrix of eigencolumns determined from $\mathbf{I}_i$.

STEP 6: Rotational adjustment is performed using the rotation matrix $\mathbf{S}_1 \, \mathbf{S}_2^{\,T}$ and the rotation formula:

$$\mathbf{I}_2 = \mathbf{S}_2 \, \mathbf{S}_1^{\,T} \, \mathbf{I}_1 \, \mathbf{S}_1 \, \mathbf{S}_2^{\,T} \tag{1.9}$$

The principal axes method has been used by various research groups, with variable results. Alpert et al.[2] used the method for three-dimensional alignment of MR data of the brain. They estimate the rotational or translational errors as the difference of the applied transformation parameter to the computed one. They reported that when the full volumes are used for the computation of the principal axes transformation, the rotational errors are less than 0.5 degrees and the translational errors less than 0.1 mm. When the surfaces are used, the errors are three to six times greater. Slomka et al.[3] used this method for three-dimensional alignment of SPECT image volumes of the heart. Their method failed to produce good rotational accuracy and they advise that it should be used as a preprocessing step to a more robust registration scheme. Toga and Banerjee[4] compared the accuracy of the method to the cross-correlation coefficient for two-dimensional registration of SPECT image scans of the brain and reported that the principal axes method often resulted in poor accuracy compared to cross-correlation based methods. They also reported that when the initial rotational error is more than 90 degrees, the method tends to register the images with 180 degrees rotational mismatch. Rusinek et al.[1] compared the performance of the method with the surface fitting algorithm for three-dimensional registration of MR images of the head. That group used the post registration distance of external fiducial markers as a measure of positional error and reported that the average errors are 1.3 mm for implementation of the method using full volumes and 4.7 mm for implementation of the method using surface outlines. These errors are 4 to 12 times greater than the errors produced by the surface fitting algorithm. In the same study it was shown that the principal axes

algorithm tends to produce large rotational errors for missing brain data and that the accuracy diminishes with larger initial misangulations. The advantages of the method are its simplicity and its speed (4-5 seconds per registration case).

1.5 Thesis overview

The purpose of this thesis is to present the application of a new automated, feature-based method of medical image registration to the solution of the problem of three-dimensional registration of MR images of the head.

Chapter II will present the main theoretical aspects of the registration method. A block diagram of the registration algorithm will be given first, followed by a detailed description of the theoretical issues related to all the main steps of the registration procedure.

Chapter III will provide a synopsis of the results from the application of the method in 200 two-dimensional and 240 three-dimensional registration experiments. Results addressing the rotational and translational accuracy of the method, its ability to perform cross-modality image registration and also the effect of the imaging resolution on accuracy will be given.

Finally, Chapter IV will provide an evaluation of the method and present areas of possible expansion and improvement.

CHAPTER II

THEORETICAL ASPECTS OF THE METHOD

2.1 Introduction

As described in Chapter I, two different approaches to the solution of the problem of medical image registration exist: the iterative approach represented by the correlation and surface matching methods and the analytic approach represented by the principal axes method. The subject of this thesis is the development of a new iterative method for three-dimensional image registration. The method developed uses a ragistration criterion, similar to the ratio image uniformity correlational criterion presented by Woods et al.[9,10]. As Chapter III will show, the modifications made to the criterion together with the new way that it is minimized, allowed the use of the surface as the main registration feature and therefore the method can no longer be characterized as correlational. A general overview of the processing steps of the method together with its main theoretical aspects will be presented in this chapter.

2.2 Processing steps of the method

To register two three-dimensional studies, the method uses the following processing steps:

I) Each of the scans of the two studies is classified with the use of the fuzzy c-means classification algorithm as presented by Bezdek et al. [22]. Three clusters are used and a threshold for each scan is computed by taking the mean value of the centers of the two lowest clusters. This threshold is the value that separates the signal from the

background area for each scan. The lowest of all the thresholds computed for each study is considered the global threshold for this study. No thresholding operation is performed at this point.

II) The two studies are interpolated using a trilinear interpolation routine to create the cubic voxel volumes. This step is necessary because of the different resolution in the xy plane and the z axis used in the acquisition of three-dimensional medical image data.

III) All the voxel values of the two volumes are compared to the global thresholds. Voxels that have signal intensities lower than the corresponding global threshold are set to zero.

IV) Finally, an iteration loop based on Chebyshev's approximation theory[24] is used to minimize the registration function, which is defined as the mean squared value of the average weighted ratio $\tilde{R}$ of the two volumes:

$$E\left(\tilde{R}^2\right) \quad \text{with} \quad \tilde{R} = \frac{1}{2} * \left(weighted(\frac{A}{B}) + weighted(\frac{B}{A}) \right) \tag{2.1}$$

where A and B are the two volumes. The ratios of the two volumes are computed on a voxel per voxel basis and weighting is performed by setting the voxel ratios with background voxels in the denominator to a standard high value. All the other voxel ratios are not affected and generally have low values.

In the next sections of this chapter, the basic theory and formulas relating to the steps

outlined above will be presented. A block diagram of the registration method is shown in figure 1.

2.3 Fuzzy c-means classification

The fuzzy c-means classification algorithm has been used in this thesis for the computation of the thresholds that define the surfaces in the two studies to be registered. The choice of this classification method was based on the results presented by Bezdek et al.[22] and Hall et al.[23], who applied the algorithm to T1 and T2 MR images. The algorithm for the implementation of this classification method is also presented in [22] and is briefly outlined below.

The purpose of the fuzzy c-means algorithm is to compute, for a given data set x[1...n], the optimal values of the centers V[1...c] of c clusters, by using the c fuzzy memberships assigned to each data element u[1...n,1...c] and by minimizing the fuzzy within-groups sum-of-squared-errors function, which is defined as:

$$J(u,x)= \sum_{k=1}^{n}\sum_{i=1}^{c}(u[i,k])^{m} D(x[k],V[i]) \qquad (2.2)$$

where D can be considered as the Euclidean distance of the data element x[k] from the center V[i] and m is a weighting exponent on each fuzzy membership. According to Bezdek and colleagues[22], J(u,x) can be minimized if and only if:

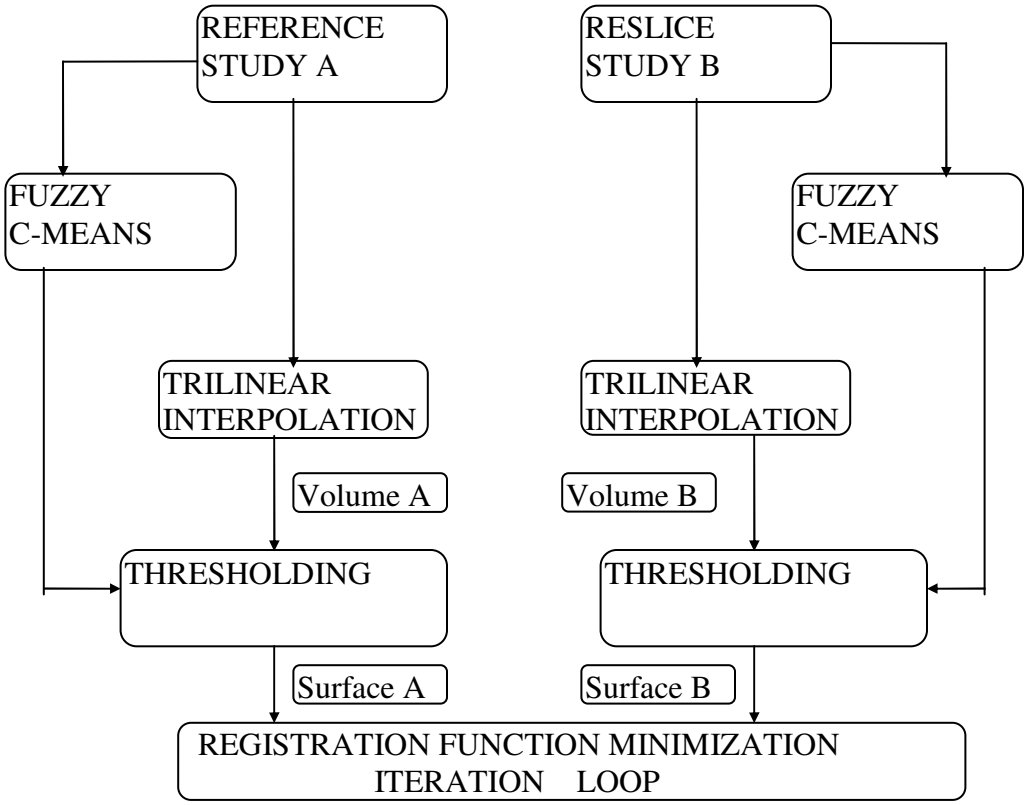

Figure 1: Block diagram of the registration algorithm.

$$u[i,k]= \left[\sum_{j=1}^{c} \left(\frac{D(x[k],V[i])}{D(x[k],V[j])} \right)^{\frac{2}{(m-1)}} \right]^{-1} \quad \text{for all i,k} \tag{2.3}$$

and $$V[i]= \frac{\sum_{k=1}^{n} (u[i,k])^m x[k]}{\sum_{k=1}^{n} (u[i,k])^m} \quad \text{for all i=1...c.} \tag{2.4}$$

The minimization can be performed using the following steps :

STEP 1: Initialize the number of clusters c, the fuzzy memberships array u[1...n,1...c], the weighting exponent m>1, the maximum number of iterations T and the error tolerance e>0. For this thesis the number of clusters is provided by the user; the membership array is initialized with crisp memberships so that each voxel has one of the c memberships equal to 1 and all the others equal to zero, m is set to 1.1, T to 100 and e to 1.

STEP 2: Compute the initial values of the c cluster centers using (2.4).

STEP 3: For t=1,2,...T, compute memberships using (2.3) and update the cluster centers array V_{t+1} using (2.4).

STEP 4: Compute $E_t = D(V_{t+1}, V_t)$

STEP 5: If $E_t < e$ stop , else next t.

The generalization of this algorithm assigns vectors instead of arithmetic values to each

voxel and it was used by Bezdek's group for classifying MR images using both T1 and T2 imaging sequences.

For the application of the algorithm in this thesis, a hierarchical form of the algorithm was implemented. In this implementation the user is able to apply the algorithm hierarchically to analyze further the highest cluster. For example, if the user chooses two levels of hierarchy with two and three clusters for each level, then the fuzzy c-means with two clusters will first be applied to all the voxels of the image and then the voxels that belong to the defuzzified highest cluster will be further analyzed with three clusters. Defuzzification is performed by using the mid distance of the centers of sequential clusters as a threshold. When one level of hierarchy is used, the method is equivalent to the fuzzy c-means algorithm as presented in [22]. An example application of the fuzzy c-means to a proton density MR scan is shown in figure 2. The left image is the original MR scan, the center image is the c-means classified and defuzzified scan with one level and three clusters, and the right image is the c-means classified and defuzzified scan with one level and 7 clusters.

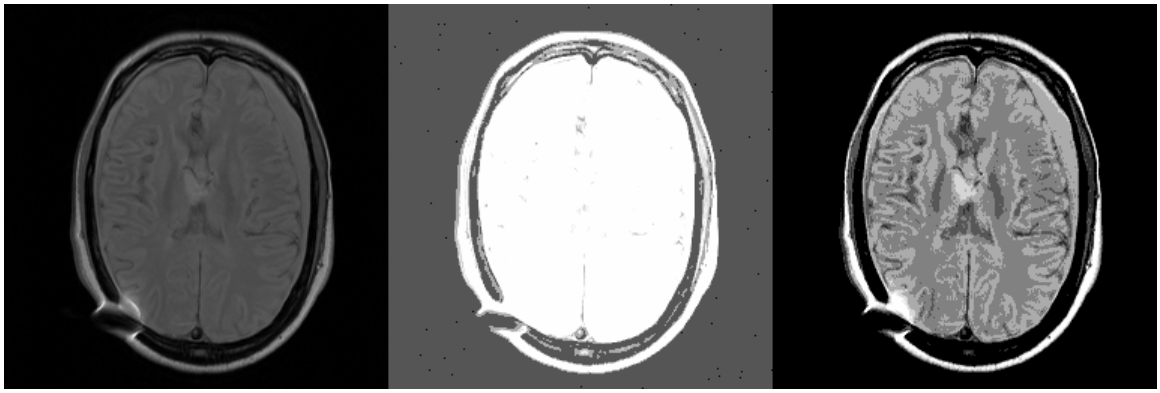

Figure 2: Application of the fuzzy c-means to an MR scan. Left: the original scan. Center: the c-means classified and defuzzified scan with c=3. Right: the c-means classified and defuzzified scan with c=7.

2.4 Trilinear interpolation

The second step of the registration method is to create the cubic voxel volumes using a trilinear interpolation routine. The formulas used for trilinear interpolation were based on the bilinear interpolation formulas presented in [25]. The interpolation procedure is as follows:

Let's consider a three-dimensional study with size LxMxN voxels and voxel size XSxYSxZS mm with XS=YS < ZS and L=M. The interpolation parameters along the three dimensions will be X_INTERP=1, Y_INTERP=1, Z_INTERP=ZS/XS. The interpolated cubic voxel volume resulting from this study will have a size of LnewxMnewxNnew with Lnew=L*X_INTERP, Mnew=M*Y_INTERP, Nnew=N*Z_INTERP. For each voxel (xnew,ynew,znew) in this volume, a signal intensity value G is computed using the formula:

$$G(x,y,z)=a*x+b*y+c*z+d*x*y+e*x*z+f*y*z+g*x*y*z+h \quad (2.5)$$

with x=xnew/X_INTERP, y=ynew/Y_INTERP, z=znew/Z_INTERP. The parameters a,b,c,d,e,f,g,h are computed by using the signal intensities G1-G8 of the eight voxels of the original study that form a cube around the (x,y,z) point. So if xint=(int)x, yint=(int)y and zint=(int)z, we have the system of 8 equations with eight unknowns a-h:

$$G1=G(xint,yint,zint) \quad (2.6)$$

$$G2=G(xint+1,yint,zint) \quad (2.7)$$

$$G3=G(xint,yint+1,zint) \quad (2.8)$$

$$G4=G(xint+1,yint+1,zint) \quad (2.9)$$

$$G5=G(xint,yint,zint+1) \quad (2.10)$$

$$G6=G(xint+1,yint,zint+1) \quad (2.11)$$

$$G7=G(xint,yint+1,zint+1) \quad (2.12)$$

$$G8=G(xint+1,yint+1,zint+1) \quad (2.13)$$

The solution of this system gives:

$$g=A+B+F-(C+D+E) \quad (2.14)$$

$$d=C-(A+B)-g*zint \quad (2.15)$$

$$f=E-B-g \quad (2.16)$$

$$e=D-A-g \quad (2.17)$$

$$a=A-d*yint-e*zint-g*yint*zint \quad (2.18)$$

$$b=B-d*xint-f*zint-g*xint*zint \quad (2.19)$$

$$c=H-e*xint-f*yint-g*xint*yint \quad (2.20)$$

$$h=G1-a*xint-b*yint-c*zint-d*xint*yint-e*xint*zint-f*yint*zint-g*xint*yint*zint \quad (2.21)$$

with :

A=G2-G1, B=G3-G1, C=G4-G1, D=G6-G5, E=G7-G5, F=G8-G5, H=G5-G1

Figure 3 shows the surface rendering of a trilinearly interpolated MR volume with interpolation parameters 1:1 along the x and y axes and 5:0.9 along the z axis.

2.5 Registration function - Iteration loop

As mentioned previously, the registration algorithm aims at minimizing the mean squared value of the average weighted ratio of the two images. The way that the registration function is computed and minimized will be presented now in greater detail.

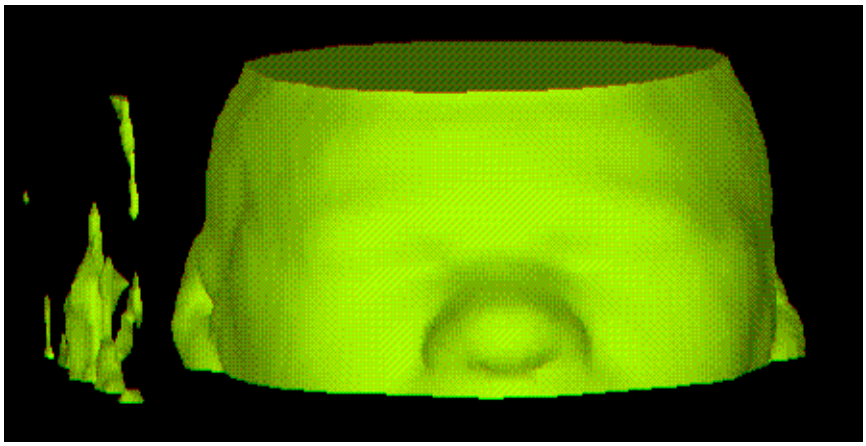

Figure 3: Surface rendering of a trilinearly interpolated cubic voxel volume. Interpolation parameters are 1:1 along the x and y axes and 5:0.9 along the z axis.

Let's consider two three-dimensional digital images $A[i,j,k]$ and $B[i,j,k]$ with i:1...L, j:1...M, k:1...N. Using these images two ratios can be defined, the ratio R_1 of image A to image B with $R_1[i,j,k] = \frac{A[i,j,k]}{B[i,j,k]}$ and the ratio R_2 of image B to image A with

$R_2[i,j,k] = \dfrac{B[i,j,k]}{A[i,j,k]}$. Let's define now as *S* an LxMxN image that results from A or B by keeping nonzero values only for the signal voxels and as *N* an LxMxN image that results from A or B by keeping nonzero values only for background voxels whose intensities are due to noise. The following equations stand $\forall$ *i:*1...L, *j:*1...M, *k:*1...N:

$$S[i,j,k] \neq 0 \Leftrightarrow N[i,j,k] = 0 \tag{2.22}$$

$$A[i,j,k] = S_A[i,j,k] + N_A[i,j,k] \tag{2.23}$$

$$B[i,j,k] = S_B[i,j,k] + N_B[i,j,k] \tag{2.24}$$

$$R_1[i,j,k] = \frac{S_A[i,j,k] + N_A[i,j,k]}{S_B[i,j,k] + N_B[i,j,k]} \tag{2.25}$$

$$R_2[i,j,k] = \frac{S_B[i,j,k] + N_B[i,j,k]}{S_A[i,j,k] + N_A[i,j,k]} \tag{2.26}$$

The weighted ratios $\tilde{R}_1$ and $\tilde{R}_2$ can now be defined as:

$$\tilde{R}_1[i,j,k] = \begin{cases} R_1[i,j,k] & \text{when } S_B[i,j,k] \neq 0 \\ C & \text{when } S_B[i,j,k] = 0 \end{cases} \tag{2.27}$$

$$\tilde{R}_2[i,j,k] = \begin{cases} R_2[i,j,k] & \text{when } S_A[i,j,k] \neq 0 \\ C & \text{when } S_A[i,j,k] = 0 \end{cases} \tag{2.28}$$

$\forall$ *i:*1...L, *j:*1...M, *k:*1...N

where *C* is a standard high value.

The function that is minimized iteratively is the mean squared value of the mean weighted ratio, that is :

$$E(\tilde{R}^2) \text{ with } \tilde{R}[i,j,k] = \frac{\tilde{R}_1[i,j,k] + \tilde{R}_2[i,j,k]}{2} \quad \forall\ i{:}1...\text{L},\ j{:}1...\text{M},\ k{:}1...\text{N} \qquad (2.29)$$

Figure 4 illustrates the meaning of the above relationships. The first line shows two MR scans that are rotated to each other by 30 degrees. The second line left shows the two scans superimposed on each other and the second line right gives a mapping of the different types of areas that can be found in the mean weighted ratio image $\tilde{R}$. In the white area, the weighted ratios $\tilde{R}_1$ and $\tilde{R}_2$ are computed using signal voxels only, whereas in the gray area, one of the ratios is computed using background voxels in the denominator and this ratio is set to a standard high value. It is obvious that the gray area does not exist for the correct registration position. For this position, the registration function gets its minimum value.

The iteration loop used for the minimization of the registration function is programmed with the following rules:

1. One of the six possible geometric transformation parameters (three rotations around the three axes and three translations along the three axes) is adjusted with each iteration. For the testing performed for this thesis, the order was set to be the rotations first,

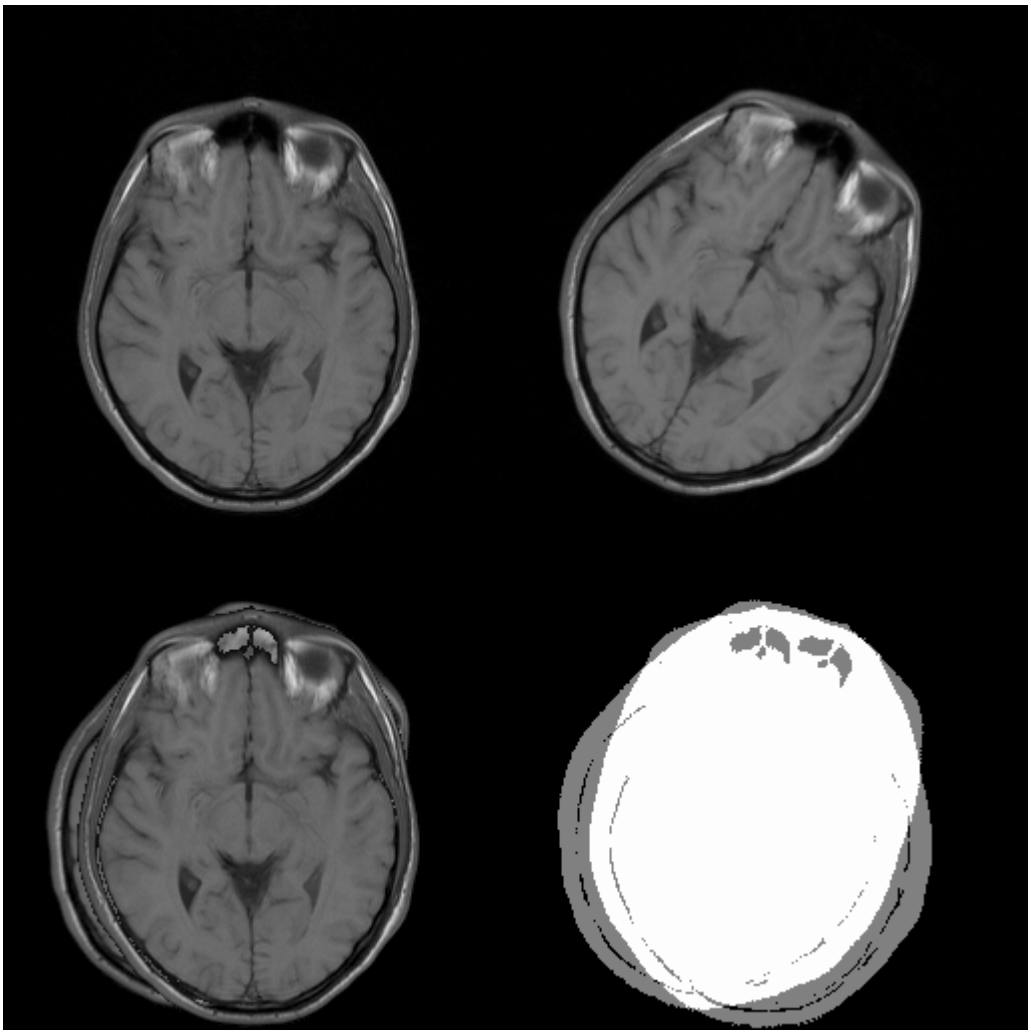

Figure 4: Illustration of the different image areas used by the algorithm for the computation of the registration function. First row: two scans rotated to each other by 30 degrees. Second row: The two scans when superimposed give two different types of area. In the white area the registration function is computed with the use of signal voxels only, whereas in the gray area both signal and background voxels are used.

followed by the translations. The reason for this order selection is that the centroid registration of the two volumes could be considered as a first step of the registration method. This step was omitted, so that the translational displacements imposed can be considered errors from the centroid registration procedure.

2. One of the two volumes is defined as the *reference* volume and the other as the *reslice* volume, which is to be aligned to the reference. Since the registration function is symmetric, the choice of the reference volume affects only the sign of the final adjustment values computed by the method.

3. For each iteration the registration function is computed for n=4 Chebyshev points per 36 transformation units. The transformation units are degrees for rotations and voxels for translations. The Chebyshev points used are[24] :

$$x_k = 18\cos\left(\frac{\pi(k-\frac{1}{2})}{n}\right) \qquad \text{k=1,...,n} \tag{2.30}$$

For all other points in the range of the 36 transformation units, the registration function is approximated using the Chebyshev approximation formula:

$$f(x) \approx \left[\sum_{k=0}^{n-1} c_k T_k(x)\right] - \frac{1}{2}c_0 \tag{2.31}$$

$T_k(x)$ is the Chebyshev polynomial of degree k and is given by the explicit formula:

$$T_k(x) = \cos(k \arccos(x)) \tag{2.32}$$

which can be given explicitly in a polynomial form as:

$$T_0(x) = 1 \tag{2.33}$$

$$T_1(x) = x \tag{2.34}$$

$$T_2(x) = 2x^2 - 1 \tag{2.35}$$

$$T_3(x) = 4x^3 - 3x \tag{2.36}$$

$$T_4(x) = 8x^4 - 8x^2 + 1 \tag{2.37}$$

...

$$T_{n+1}(x) = 2xT_n(x) - T_{n-1}(x) \qquad n \geq 1 \tag{2.38}$$

The coefficients c_k are the Chebyshev coefficients and are defined by

$$c_k = \frac{2}{n}\sum_{l=1}^{n} f(x_l)T_k(x_l) \quad k=0,...,n-1 \tag{2.39}$$

where x_l are the Chebyshev points.

The minimum of the approximated registration function is considered as the adjustment value for the geometric transformation parameter.

4. A transformation parameter is determined to have converged when it completes two iterations that give adjustment values less than one transformation unit.

5. A maximum number of eight iterations per transformation parameter is allowed. If the parameter has not converged after eight iterations, the adjustment value is considered to be the average of the adjustment values given by the seventh and eighth iteration. In this study we found that in all the cases of non-convergence, the adjustment values oscillated around the correct registration position with amplitudes greater than one transformation unit.

The results from the application of the above algorithm to a total of 200 two-dimensional and 240 three-dimensional registration experiments will be presented in the next chapter.

CHAPTER III

EXPERIMENTAL PROTOCOLS AND RESULTS

3.1 Introduction

The method presented in the previous chapter was applied to solve the problem of registration of MR images of the head. A total of 200 two-dimensional and 240 three-dimensional registration experiments were performed using patient data from the database of the Cleveland Clinic Foundation. The purpose of this chapter is to present the protocol used for these experiments and also to provide a synopsis of the main results obtained.

3.2 Data protocol

The MR data used came from 10 different patients with various diseases. The data had the following characteristics:

a) The patients had repetitive MR examination at two different times. The examination data can be found in Appendix A.

b) For each time, T1- and T2-weighted axial interleaved studies that corresponded to the same position of the patient's head were performed.

c) All the studies had 19 scans.

d) All the studies had xy-plane resolution of 0.9 mm and z-axis resolution of 5 mm.

3.3 Protocol for 2D experiments - "20 displacement" technique

Using the data described in the previous section, a total of 200 two-dimensional experiments for alignment of a T2 to a T1 axial scan were performed. These experiments will be referred to as *"20 displacement"* experiments and were conducted according to the following rules:

a) For each patient the tenth scan of each of the T1 and T2 studies of the first examination time were used.

b) The T1 scan was used as the reference scan. The T2 scan was considered the reslice scan. The latter was rotated and translated using a standard set of 20 two-dimensional geometric transformations and then registered to the reference scan, giving 20 registration experiments per patient. The geometric transformations parameters were randomly selected using a random number generator in the range of -45 to +45 degrees for the xy rotation and -30 to +30 voxels for x and y translations. The translations were rounded to the nearest integer for reasons that relate to the implementation of the geometric transformations routine; these will be explained later in this chapter. The resulting "20 displacement" set is shown in table 1.

c) All the experiments were performed at full resolution. The size of the scans in voxels was 256x256 and the voxel size was 0.9 mm.

Table 1 : Geometric transformation set used for the two-dimensional "20 displacement" registration experiments.

Transformation #	xy - rotation (degs)	x-translation(voxs)	y-translation(voxs)
1	-40.08	7	0
2	21.37	-9	-19
3	-16.18	-10	-11
4	-34.80	-5	2
5	-2.67	10	27
6	-32.64	-6	-20
7	-14.40	-17	12
8	-36.15	0	-16
9	33.23	-26	0
10	20.60	16	-23
11	-25.82	24	-25
12	-37.63	-23	-7
13	8.17	26	-13
14	7.09	12	-8
15	-44.71	0	29
16	24.54	29	2
17	-36.06	-5	16
18	-28.42	-19	9
19	15.82	13	16
20	0.35	-5	17

d) The *Absolute Error (AE)* per transformation parameter was defined as the absolute difference of the adjustment value from the applied transformation parameter value. The xy rotation AE for each transformation was defined as the *Absolute Rotational Error (ARE)* for the transformation and was computed in degrees. The *Absolute Translational Error (ATE)* per transformation was computed in millimeters by

averaging the x and y translation AEs in voxels and then by multiplying the average value with the voxel size (0.9 mm). The *Average Absolute Rotational Error (AARE)* per patient was defined as the average of the AREs from all the transformations. Similarly, the *Average Absolute Translation Error (AATE)* per patient was defined as the average of the ATEs from all transformations.

3.4 Protocol for 3D experiments

The three-dimensional registration accuracy of our method was tested with a total of 240 three dimensional registration experiments. Two types of three-dimensional experiments were performed: The *"10 displacement"* experiments, a three-dimensional version of the "20 displacement" experiments, and the *"different times"* experiments.

For the "10 displacement" experiments the following rules were used:

a) For each patient the T1 and T2 studies of the first examination date were used.

b) The T1 study was used as the reference study.The same study was also rotated and translated using a standard set of 10 three dimensional geometric transformations and then registered to the reference study, giving 10 T1-T1 three-dimensional registration experiments per patient. The T2 study was also rotated and translated using the same three-dimensional geometric transformation set and then registered to the reference study, giving 10 T1-T2 three-dimensional registration experiments per patient. The rotational parameters of the geometric transformation set were randomly chosen within the limits of the adjustment values that were obtained from registration of patient data from different times. The translational parameters were kept within lower limits than those resulting from "different times" experiments, because they simulate centroid registration errors.

The limits used were -30 degrees to +30 degrees for xy rotation, -10 degrees to +10 degrees for yz and zx rotations, -10 to +10 mm for x and y translations and -5 to +5 mm for z translation. The translations were converted to voxels by dividing the millimeters with the cubic voxel size and quantizing to the nearest integer. The resulting set of the 10 three-dimensional geometric transformations is shown in table 2.

c) All the experiments were performed at half resolution using a voxel size of 1.8 mm.

d) The *Absolute Error (AE)* per transformation parameter was defined as the absolute difference of the adjustment value from the applied transformation parameter value. The average of the AEs for xy, yz, zx rotations was defined as the *Absolute Rotational Error (ARE)* per transformation and was computed in degrees. The *Absolute Translational Error (ATE)* per transformation was computed in millimeters by averaging the x, y and z translation AEs in voxels and then by multiplying the average value with the voxel size (1.8 mm). The *Average Absolute Rotational Error (AARE)* per patient was defined as the average of the AREs from all the transformations. Similarly, the *Average Absolute Translation Error (AATE)* per patient was defined as the average of the ATEs from all transformations.

Table 2: Geometric transformation set used for the "10 displacement" registration experiments

Transfor-mation #	xy rotation (deg)	yz rotation (deg)	zx rotation (deg)	x translation (mm)	y translation (mm)	z translation (mm)
1	-10.26	-6.94	-9.3	-9.2	-3.6	-3.98
2	12.42	2.32	-3.7	-4.6	-9.6	-2.02
3	-8.58	-4.38	1.9	8.4	6.9	-4
4	19.26	-7.2	-1.9	-1.66	-8	1.97
5	-26.58	-6.3	-2.16	-3.2	-7.6	0
6	7.56	2.1	-7.6	0	-6.08	0.8
7	-5.82	-2.2	2.8	-8.4	-5.72	2
8	-5.04	4.2	-4.04	4.2	3	-2
9	-15.66	-5.14	6.04	8	-6.04	1.6
10	-9.24	6.44	-6.7	-0.5	1.48	3.2

The "different times" experiments were performed in the following way:

a) For each patient the T1 study of the first examination date and the T1 and T2 studies of the second examination date were used.

b) The T1 study of the first examination date was considered as the reference study. The T1 and T2 studies of the second examination date were considered as the reslice studies and were both registered to the T1 study of the first examination date.

c) The experiments were performed first at half and then at full resolution, giving four "different times" registration experiments per patient.

3.5 Nearest neighbor - Quantization effects

As already noted, the registration algorithm moves the reslice image at positions that are defined by the Chebyshev points, computes the registration function values for these points and then extrapolates its values for all the other points using the Chebyshev approximation formulas. The implementation of this algorithm requires the use of a geometric transformation routine that incorporates a trilinear interpolation step that will ensure the floating point operations. For all the testing performed for this thesis, a geometric transformations routine that follows the nearest-neighbor rule for coordinate computations was used. This choice was based solely on the non-time-efficient programming of a combined geometric transformation and trilinear interpolation routine.

The effects of this choice on the performance of the algorithm are as follows:

a) When rotations are present, the nearest-neighbor approach generates voxels within the signal area for which no values are computed. These voxels are crucial to the performance of the algorithm because they are considered as background points. The solution to this problem was given by putting an additional loop at the end of the geometric transformation routine that detects these voxels and computes a value for them by interpolating linearly between the neighboring voxels. Figure 5 illustrates this effect for the case of a two-dimensional image. The left image is the original MR scan. The center image is the scan rotated by 30.5 degrees with the nearest-neighbor artifact present. The right image shows the same rotated scan after interpolation.

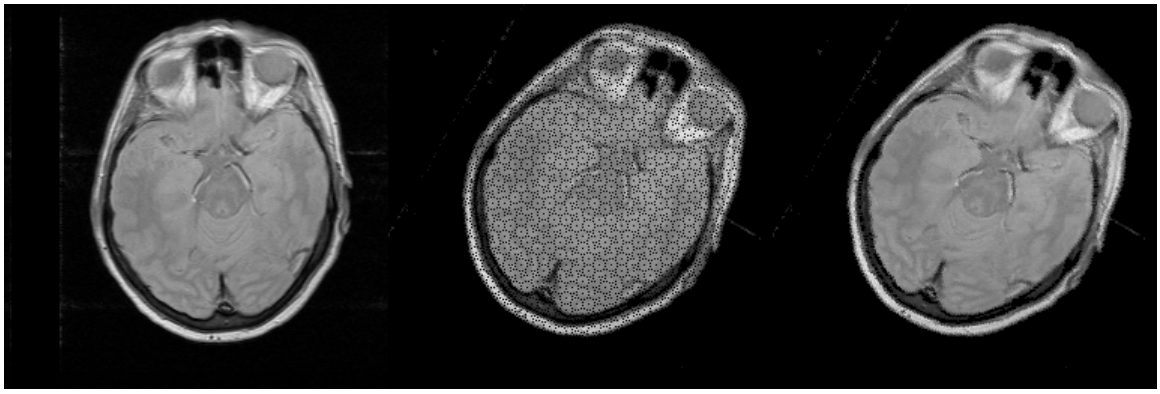

Figure 5: Use of the linear interpolation for the implementation of the geometric transformations. Left: original MR scan. Center: MR scan rotated by 30.5 deg using the nearest-neighbor rule for the geometric transformations. Right: MR scan rotated by 30.5 deg after the implementation of linear interpolation.

b) When translations are present, the effects of the quantization imposed by the nearest-neighbor approach are more serious. First, the translation points for which the computation of the registration function is done are not the Chebyshev points but the nearest integers to these points. Second, the adjustment value for each translation iteration loop is not the minimum of the registration function but the nearest- nteger to this minimum. We were not able to define the effect of these two events on the accuracy of the method for translational adjustments. For this reason, in all the experiments performed for this thesis, the comparisons relating to the accuracy of the method use only the rotational errors.

3.6 Two-dimensional results - "20 displacement" technique

3.6.1 Choice of the number of Chebyshev points

For all the two-dimensional experiments performed, the number of Chebyshev points

was set to n=10 for 36 transformation units. This value was decided by applying the "20 displacement" technique experiment for patient 1 for n=4,5,...,10 and using only the geometric transformations 1-10. The Average Absolute Rotational Error for each value of n is given in table 3. It was less than 1 degree for $n \geq 8$. Using these results, the value of n was set to 10.

Table 3: Average Absolute Rotational Errors for the two-dimensional T1-T2 MR image registration case for patient 1 and various numbers of Chebyshev points n for 36 transformation units.

Chebyshev points n	4	5	6	7	8	9	10
AARE (degrees)	3.85	3.47	3.01	1.27	0.21	0.36	0.17

3.6.2 Choice of the registration function - Variance versus mean squared value

As described in Chapter II, the registration function is defined as the mean squared value of the average weighted ratio of the two images. The initial implementation of the method used a different registration function - the variance of the average weighted ratio. The variance of the ratio is also the correlational criterion that Woods et al.[9,10] use to align images. The mean squared value was chosen for two reasons:

a) The variance function gets a small value for the correct registration position but its global minimum is for the position in which no overlap between the two images exists for which it becomes zero.

b) The registration accuracy with the mean squared value as the registration function was found to be better than with the variance. This was tested for the two-dimensional case by applying the "20 displacement" experiment for patient 1 with both the variance and the mean squared value, using only the first 10 of the 20 geometric transformations. The Absolute Rotational Error for these 10 cases with the use of the variance function varied between the values of 0.1 and 1.03 degrees (average 0.35 degrees), whereas with the use of the mean squared value, the error varied between 0.02 degrees and 0.6 degrees (average 0.17 degrees). It must be noted, however, that with the use of variance in no case were the eight iterations reached for the adjustment of any geometric transformation parameter, whereas with the mean squared value, this happened once for xy rotation, three times for y translation and four times for x translation. The Average Absolute Translational Errors were 0.9 mm for the mean squared value and 0.63 mm for the variance.

3.6.3 A two-dimensional registration example

To illustrate the registration procedure, a two-dimensional registration "20 displacement" experiment will be given in terms of the registration function curves, as they are extrapolated for the xy plane rotation parameter and for each iteration. The experiment uses the transformation number 12 and data from patient 1. The thresholds used for the two scans were computed by applying the fuzzy c-means to the two scans and were 381 for the T1 and 120 for the T2 scan. Figure 6 shows the two scans before and after registration. The top left image is the T1 reference scan, the top right image is the T2 reslice scan before registration and the bottom left image is the reslice scan after

registration. The errors computed for this experiment were 0.05 deg for xy rotation and 0 voxels for x translation and 2 voxels for y translation. Figures 7 to 9 show the variance curves with each iteration for rotational adjustment. The minimum values marked on the curves are the adjustment values that the algorithm uses to register the two images. The total adjustment is 37.68 deg, which corresponds to an error of 0.05 deg.

3.6.4 Summary of the results from 200 two-dimensional experiments

A total of 200 "20 displacement" experiments were performed using the data from the 10 patients. Table 4 gives a summary of the Average Absolute Errors per patient. It can be seen that the Average Absolute Rotational Error varies between 0.16 and 0.38

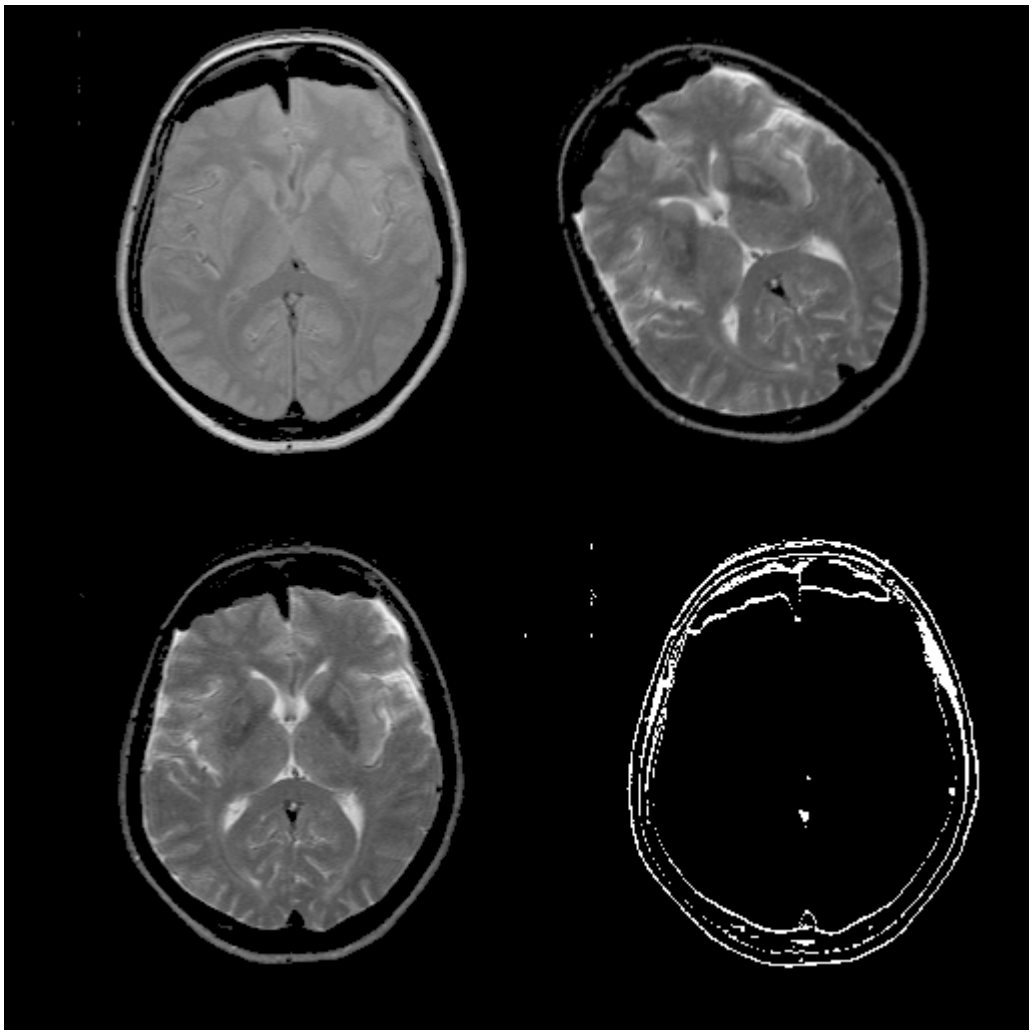

Figure 6: “20 displacement” T1-T2 registration example. Reference and reslice scans before and after registration. Top left: Reference T1 MR scan. Top right: Reslice T2 MR scan before registration. The two scans are rotated by 37.63 deg and translated by 23 voxels along the x-axis and 7 voxels along the y-axis. Bottom left: Reslice scan after registration. The registration error is 0.05 deg for xy rotation, 0 voxels for the x translation, and 2 voxels for the y translation. Bottom right: the white areas show the areas of non-overlap of the two scans after registration.

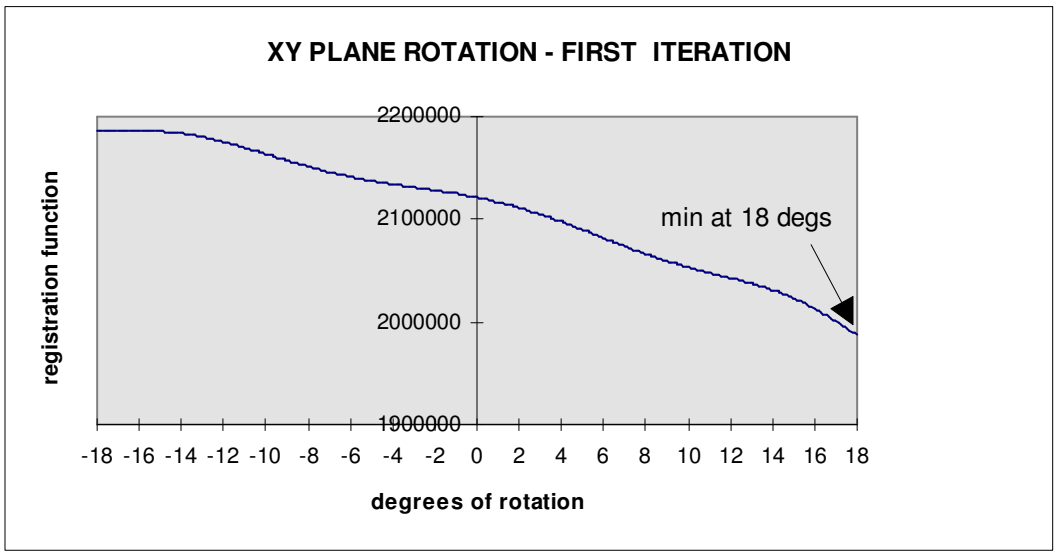

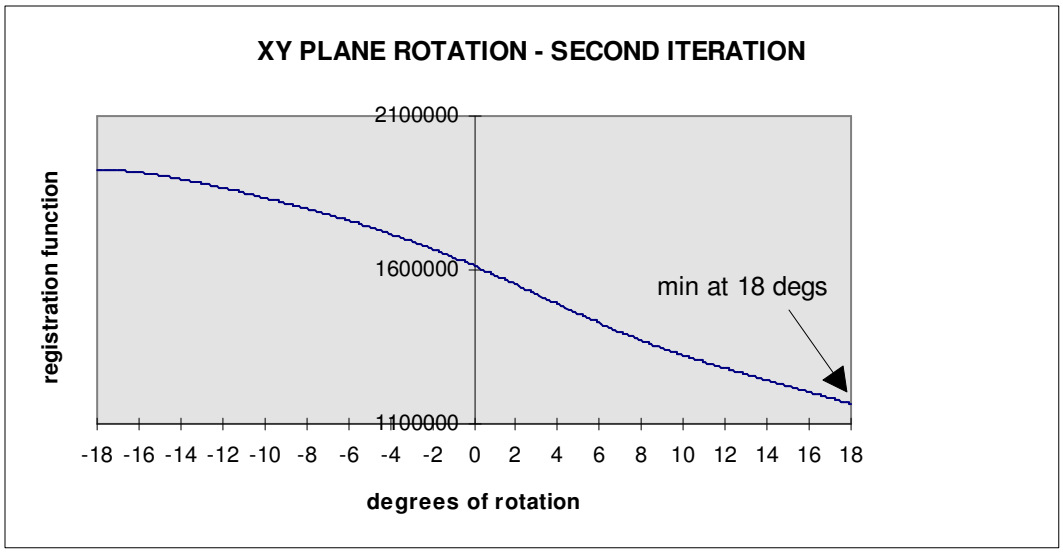

Figure 7: “20 displacement” T1-T2 registration example. Registration function minimization curves. Iterations 1 and 2.

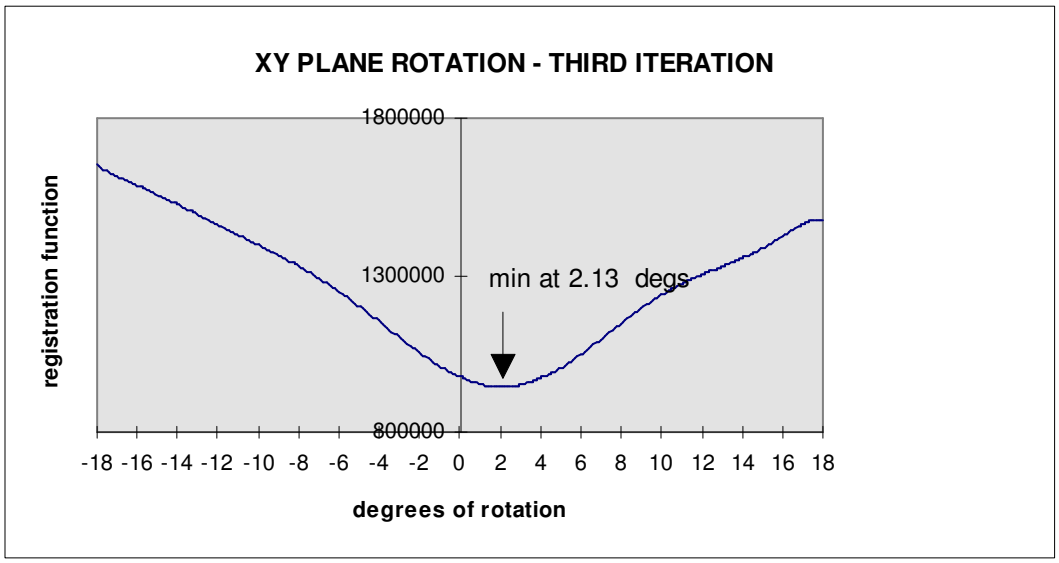

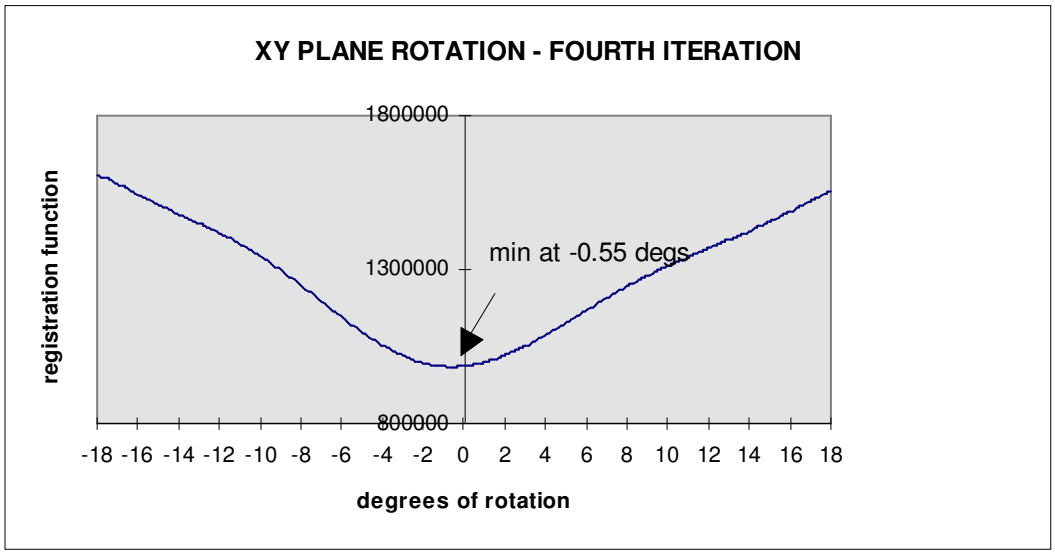

Figure 8:"20 displacement" T1-T2 registration example. Registration function minimization curves. Iterations 3 and 4.

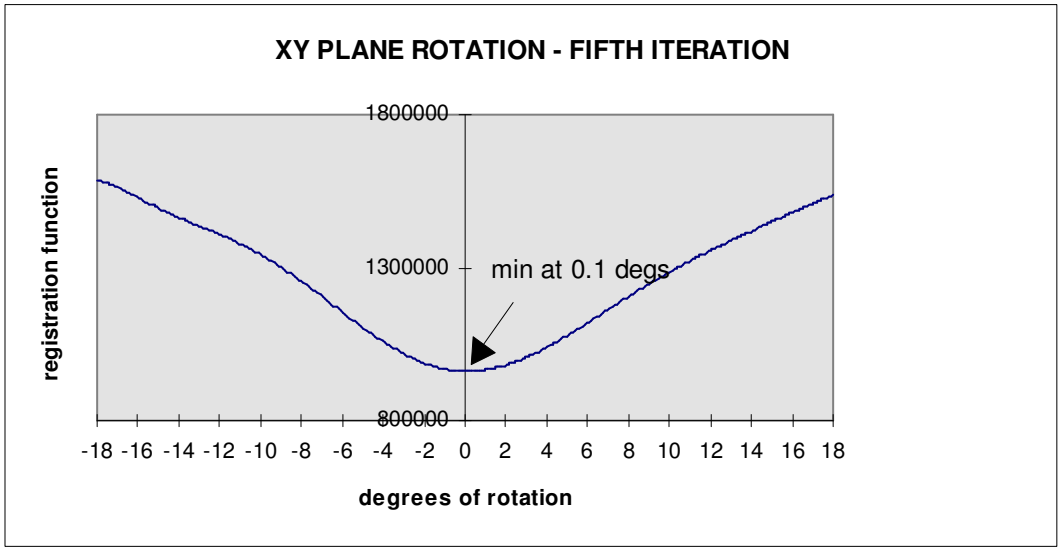

Figure 9: "20 displacement" T1-T2 registration example. Registration function minimization curve. Final iteration 5.
Total adjustment: 18+18+2.13-0.55+0.1 = 37.68 deg
Registration error: 37.68-37.63 = 0.05 deg

Table 4: Average Absolute Rotational and Translational Errors per patient for two-dimensional "20 displacement" registration experiments.

Patient number	**AARE (deg)**	**AATE(mm)**
1	0.18	0.9
2	0.21	0.9
3	0.38	0.78
4	0.25	0.32
5	0.16	0.45
6	0.19	0.9
7	0.22	0.9
8	0.25	0.9
9	0.19	0.9
10	0.25	1.01
Average	**0.23**	**0.79**

degrees (average 0.23 degrees), whereas the Average Absolute Translational Error varies between 0.32 and 1.01 mm (average 0.79 mm).

3.7 Three-dimensional results - "10 displacement" experiments

As mentioned earlier in this chapter, the "10 displacement" technique was used for performing 200 three-dimensional registration experiments for T1-T1 and T1-T2 MR data registration. For all these experiments, n=4 Chebyshev points for 36 transformation units were used because this value was found to give rotational errors less than 1 degree. This section will summarize the results obtained from these experiments. The 10 T1-T2 registration cases with the highest Absolute Rotational Errors will first be presented. Then the worst case will be selected and the whole registration procedure will be described and given in terms of surface renderings with the relative positions of the two volumes. Finally, a statistical description of the results will be given. Full results from all the "10 displacement" experiments can be found in Appendix A. They include the errors computed for each experiment and for each geometric transformation parameter.

3.7.1 Worst-case analysis

Table 5 shows the 10 worst "10 displacement" T1-T2 registration cases in terms of the Absolute Rotational Errors computed for these cases. The first column shows the order of the case with case 1 corresponding to the experiment with the highest ARE. The second and third columns show the patient and the geometric transformation numbers. The fourth column shows the ARE values for each case, and the fifth column shows

Table 5: Absolute Rotational Errors for the 10 worst cases of T1-T2 "10 displacement" registration experiments.

Case	Patient	Transformation	ARE (degrees)	AARE (degrees)
1	3	5	0.89	0.46
2	6	5	0.80	0.45
3	3	3	0.79	0.46
4	10	3	0.75	0.49
5	6	3	0.70	0.45
6	8	4	0.70	0.44
7	4	3	0.69	0.27
8	8	10	0.66	0.44
9	3	4	0.65	0.46
10	1	4	0.61	0.36

the Average Absolute Rotational Error for the patient of the second column. The worst case corresponds to patient 3 and transformation 5, which gave an ARE value of 0.89 degrees, 0.43 degrees higher than the AARE value for patient 3.

Table 6 shows the errors for all the transformation parameters and iterations for the worst-case experiment. The first column shows the iteration numbers with iteration number 0 corresponding to the initial misalignments imposed by transformation 5.

Columns 2 to 7 show the errors for each iteration and transformation parameter. The last row of the table shows the final adjustment errors. The application of the maximum iteration rule affected the adjustment errors for the xy rotation and the y translation that did not converge after eight iterations. The values of table 6 can be compared with the values of table 7, which gives the average absolute errors per iteration for all the T1-T2 "10 displacement" registration experiments that used transformation 5. This comparison shows that for the worst case there is a slowing in the rhythm of reduction of the absolute error with each iteration. This is most obvious for the xy rotation, which gives an absolute error less than 1 degree for the first time on the eighth iteration. In no other case in all the T1-T2 "10 displacement" registration experiments did a transformation parameter give error less than one transformation unit so late in the registration procedure. A similar behavior is observed for the xy rotation in the corresponding T1-T1 "10 displacement" experiment. Another interesting observation can be made

Table 6 : Errors for each iteration for the worst-case T1-T2 “10 displacement” registration experiment.

Iteration number	**xy rotation error (degrees)**	**yz rotation error (degrees)**	**zx rotation error (degrees)**	**x translation error (voxels)**	**y translation error (voxels)**	**z translation error (voxels)**
0	-26.58	-6.3	-2.16	-2	-4	0
1-6	-22.86	-3.03	-1.26	-1	2	0
7-12	-19.71	0	-0.36	2	-1	0
13-18	-16.11	0.11	-0.36	-2	-1	0
19-24	-12.63	-0.78	-0.36	1	1	0
25-30	-9.7	-0.78	-0.36	0	-2	0
31-36	-5.54	-0.78	-0.36	0	0	0
37-42	**-2.5**	-0.78	-0.36	0	**-1**	0
43-48	**-0.59**	-0.78	-0.36	0	**0**	0
Max iteration rule	**-1.54**	-0.78	-0.36	0	**0**	0

Table 7: Average Absolute Errors for each iteration of transformation 5 and all patients for T1-T2 "10 displacement" registration experiments.

Iteration number	**xy rotation error (degrees)**	**yz rotation error (degrees)**	**zx rotation error (degrees)**	**x translation error (mm)**	**y translation error (mm)**	**z translation error (mm)**
0	26.58	6.3	2.16	2*1.8	4*1.8	0
1-6	21.2	1.7	0.69	0.6*1.8	2.2*1.8	0.1*1.8
7-12	14.65	0.88	0.88	1.5*1.8	1*1.8	0.1*1.8
13-18	8.8	0.36	0.64	0.5*1.8	0.6*1.8	0.2*1.8
19-24	4.59	0.64	0.52	0.7*1.8	0.6*1.8	0.2*1.8
25-30	2.28	0.33	0.65	0.3*1.8	0.5*1.8	0.2*1.8
31-36	1.24	0.52	0.5	0.2*1.8	0.3*1.8	0.2*1.8
37-42	0.51	0.37	0.49	0.2*1.8	0.4*1.8	0.2*1.8
43-48	0.44	0.5	0.49	0.2*1.8	0.2*1.8	0.2*1.8
Max iteration rule	0.55	0.5	0.49	0*1.8	0.2*1.8	0.2*1.8

when the same values with table 7 are computed for the T1-T1 registration experiments (table 8) and the absolute differences of the values of tables 7 and 8 are computed (table 9). It can be seen that the differences in the errors per iteration are always less than one transformation unit with an average value less than 0.5 transformation unit and the

differences in the final adjustment are also less than 0.5 transformation unit. This result shows that our method is not affected by the differences in the signal intensities between the two studies and can thus be considered surface based. More results that justify this characterization will be given later in this chapter.

3.7.2 Worst T1-T2 "10 displacement" registration case

As stated in the previous section, the worst case for T1-T2 "10 displacement" registration corresponds to patient 3 and transformation 5. The errors after each iteration for this case were given in table 6 and the ARE was computed to be 0.89 degrees, which was 0.43 degrees higher than the AARE value for the same patient and all 10 transformations of table 2. In this section the whole registration procedure for this case will be presented in detail and will also be depicted with surface renderings of the two volumes before and after registration.

For the worst-case experiment, the T1-T2 interleaved study of patient 3 of the first examination date (November 3, 1994) was used. This study constituted of 19 T1 and 19 T2 scans with voxel size 0.9x0.9x5 mm. The files were transformed from ACR-NEMA 2.0 format to the Cleveland Clinic Foundation Biomedical Engineering

Table 8: Average Absolute Errors for each iteration of transformation 5 and all patients for T1-T1 "10 displacement" registration experiments.

Iteration number	**xy rotation error (degrees)**	**yz rotation error (degrees)**	**zx rotation error (degrees)**	**x translation error (mm)**	**y translation error (mm)**	**z translation error (mm)**
0	26.58	6.3	2.16	2*1.8	4*1.8	0*1.8
1-6	21.44	1.76	0.63	0.7*1.8	2.1*1.8	0*1.8
7-12	13.97	0.85	1	1.9*1.8	0.6*1.8	0*1.8
13-18	9.44	0.6	0.47	0.8*1.8	0.3*1.8	0*1.8
19-24	4.63	0.52	0.97	0.6*1.8	0.5*1.8	0*1.8
25-30	2.24	0.33	0.51	0.5*1.8	0.3*1.8	0*1.8
31-36	0.97	0.27	0.48	0.4*1.8	0.3*1.8	0*1.8
37-42	0.58	0.26	0.44	0.3*1.8	0.3*1.8	0*1.8
43-48	0.34	0.26	0.33	0.3*1.8	0.3*1.8	0*1.8
Max iteration rule	0.4	0.32	0.34	0.1*1.8	0.1*1.8	0*1.8

Table 9: Absolute differences of the errors given in tables 7 and 8.

Iteration number	xy rotation error (degrees)	yz rotation error (degrees)	zx rotation error (degrees)	x translation error (mm)	y translation error (mm)	z translation error (mm)
0	0	0	0	0*1.8	0*1.8	0*1.8
1-6	0.24	0.06	0.06	0.1*1.8	0.1*1.8	0.1*1.8
7-12	0.68	0.03	0.12	0.4*1.8	0.4*1.8	0.1*1.8
13-18	0.64	0.24	0.17	0.3*1.8	0.3*1.8	0.2*1.8
19-24	0.04	0.12	0.45	0.1*1.8	0.1*1.8	0.2*1.8
25-30	0.04	0	0.14	0.2*1.8	0.2*1.8	0.2*1.8
31-36	0.27	0.25	0.02	0.2*1.8	0*1.8	0.2*1.8
37-42	0.07	0.11	0.05	0.1*1.8	0.1*1.8	0.2*1.8
43-48	0.1	0.24	0.16	0.1*1.8	0.1*1.8	0.2*1.8
Max iteration rule	0.15	0.18	0.15	0.1*1.8	0.1*1.8	0.2*1.8
Average	0.27	0.12	0.15	0.19*1.8	0.13*1.8	0.18*1.8

Department BIP format using the STACR utility of the BIP library. The info on the voxel size was extracted from the header of the BIP files, the raw data were also extracted, the T1 scans were separated from the T2 scans and saved as two different studies in the IMPACT raw format that is read by the all the three-dimensional image

processing programs written for this thesis. This format saves the MR scans as short raw images with a header of 6144 bytes. The size of the image data is 256x256 voxels and two bytes per voxel are used. The names of the files are descriptive and follow a standard naming format. The first character of the file name is the "i" referring to the IMPACT format followed by the patient number, the date of the examination, the number of the ACR-NEMA study and the type of the IMPACT study, the increasing number of the scan in this study and finally the ".ima" ending. For example, the name "ipat03_nov94_std0t1_10.ima" refers to an IMPACT image that corresponds to the tenth T1 scan of the first MR T1-T2 interleaved study, performed to patient 3 in November 1994. All the scans of the two IMPACT studies are saved to a standard directory "~/3d/data" from which all the three-dimensional image processing utilities read the input files. The user defines the input files by providing the standard part of the two file names, which for this example were "ipat03_nov94_std0t1_" and "ipat03_nov94_std0t2_", and also the numbers of the first and last scan of the two studies, which for a study with 19 scans would be 1 and 19.

The first program to be applied in this example registration procedure was the fuzzy c-means hierarchical algorithm. The algorithm was applied sequentially to all the scans of the two studies. For each study the classification program was executed in the following way:

The user was noted to provide two identification numbers of the first and second study. Since one study was processed with each execution of the program the same identification, for example, "ipat03_nov94_std0t1_", was used for both studies. The study to be processed had 19 scans and when the numbers of the first and last scan for the

two studies were requested, the numbers 1-10 and 11-19 were given. In this way all the scans of the IMPACT study "ipat03_nov94_std0t1_" were processed in the order 1,11,2,12,3,13.... The reason for this special type of input used by the classification algorithm is that the hierarchical form of the c-means was programmed for processing of MR FLAIR image data that are acquired in the Department of Radiology of the Cleveland Clinic Foundation; these image studies have to be read in an interleaved way. The next information that the user was asked to provide was the prefix of the names of the classified image files which were saved with a name, using this prefix followed by a number that showed the order by which the scans had been processed. Consequently the user gave the number of levels of the hierarchical scheme, which for this case was 1 and the number of clusters for the first level, which was 3. After all this information was provided, the classification program processed all the scans of the IMPACT study "ipat03_nov94_std0t1_" and computed the centers of the three clusters for each scan. These centers were then used to compute the thresholds for each scan by taking the average of the two lowest clusters centers. The same procedure was then repeated for the IMPACT study "ipat03_nov94_std0t2_". The thresholds computed for the two studies of the worst-case example are shown in Table 10. The lowest of the thresholds for each study was considered as the global threshold of the study and appears in the same table in boldface characters.

The next step of the method was to enter the main registration procedure. The user defined the two studies to be registered by giving the identification numbers of the two studies, which for this case were "ipat03_nov94_std0t2_" for the reslice study and "ipat03_nov94_std0t1_" for the reference study. The user was then asked to provide

some initial estimates for the geometric transformation parameters needed for registration. For the case of the "10 displacement" experiments, where the two studies correspond to the same position of the head, the estimates given in this point of the procedure are used to deregister the two volumes. Therefore for this experiment the rotational and translational parameters of the transformation 5 were given. Then the user was asked to provide the voxel size parameters, which were 0.9 mm for the xy plane resolution and 5 mm for the z axis thickness. Since half resolution is used for all the "10 dispacement" experiments, the xy plane resolution was multiplied by two. Using this xy plane resolution as the cubic voxel size, the translations, given in millimeters, were transformed into voxel numbers using the nearest integer approach. The trilinear interpolation routine was then applied to the two studies to create the cubic voxel with dimensions 1.8x1.8x1.8 mm. The size of the volumes created was 128x128xZ with Z=18x(5/1.8)=50. An empty area on the top and the bottom of each volume was also created by inserting (int)(5/1.8)+1=3 layers of zero valued cubic voxels. The

Table 10: Thresholds computed with the use of the fuzzy c-means for all the scans of the two studies of the worst-case T1-T2 "10 displacement" registration experiment.

Scan number	T1 study thresholds	T2 study thresholds
1	410	143
2	396	138
3	383	128
4	376	130
5	369	135
6	372	130
7	500	245
8	540	250
9	535	256
10	544	258
11	434	265
12	325	265
13	354	260
14	350	238
15	362	154
16	370	143
17	350	116
18	316	101
19	**265**	**75**

purpose was to reduce the truncation of the edges of the volume, which when the volume is rotated, exceed the image area.

After the two cubic voxel volumes were created, the main registration procedure started. First the global thresholds that were computed with the fuzzy c-means were used to set the background voxels to zero. The registration function minimization

iteration loop was then applied. Six buffers that summate the adjustment values for each of the six rotational or translational parameters were defined; their values were used to transform the reslice volume. This operation for the first iteration deregistered the two volumes with the rotational and translational parameters of transformation 5. For each of the next iterations the adjustment values were the ones computed by the iteration loop; these were used to register the two volumes. All the transformations were performed to the reslice volume, with center of rotations its centroid, which was computed before the iteration loop and was updated according to the translations applied to this volume. As noted in Chapter II, one geometric transformation parameter was adjusted with each iteration and the adjustment value was computed by taking the minimum of the registration function approximated from n=4 Chebyshev points for 36 transformation units. After all the transformations converged or the maximum iteration limit was reached, the final adjustment was applied to the reslice volume and the two volumes were saved. Figures 10 to 12 show the surface renderings with the relative position of the two volumes of the worst-case example before and after registration. For these illustrations

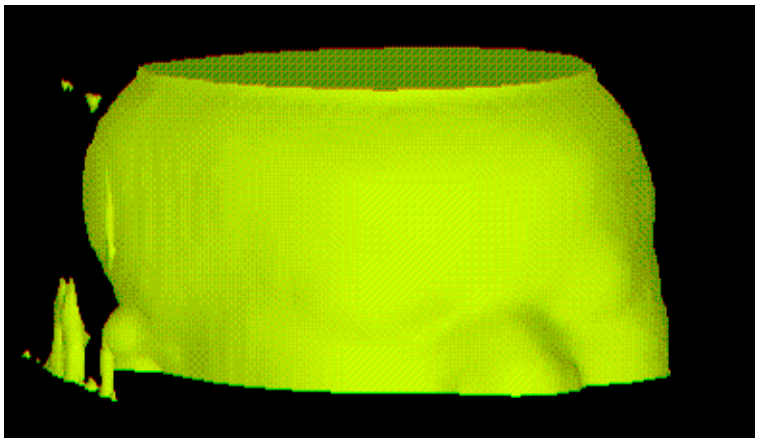

Figure 10: T1-T2 registration example. Surface rendering of the reference T1 image volume for the worst-case T1-T2 “10 displacement” registration experiment.

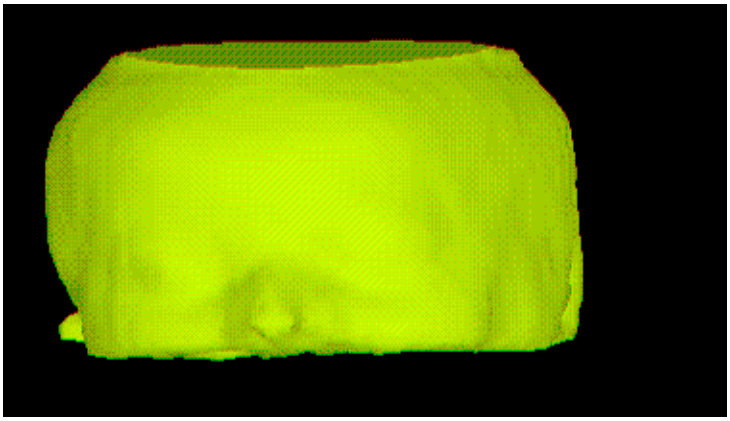

Figure 11: T1-T2 registration example. Surface rendering of the reslice T2 image volume for the worst-case T1-T2 “10 displacement” registration experiment before registration.

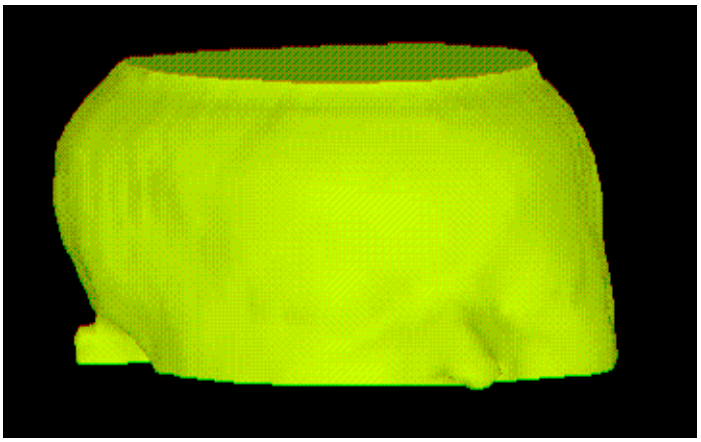

Figure 12: T1-T2 registration example. Surface rendering of the reslice T2 image volume for the worst-case T1-T2 "10 displacement" registration experiment after registration to volume of figure 10.

the two volumes were enhanced using three-dimensional median filtering and then rendered using an AVS commercial isosurface renderer.

3.7.3 Summary of the results from 200 "10 displacement" 3D experiments

A total of 200 "10 displacement" experiments were performed for T1-T1 and T1-T2 three-dimensional registration. Tables 11 and 12 give a summary of the average absolute errors per patient for "10 displacement" registration. Table 11 shows that for T1-T1 registration the Average Absolute Rotational Error per patient varied between 0.17 and 0.42 degrees with an average value of 0.24, whereas the Average Absolute Translational Error per patient varied between 0 and 0.03 voxels with an average value of 0.02. Table 12 shows the same errors for the T1-T2 "10 displacement" experiments. The average values are 0.36 for AARE (range, 0.23 to 0.49 degrees) and 0.2 voxels for AATE (range,

Table 11: Average Absolute Rotational and Translational Errors per patient for "10 displacement" T1-T1 registration experiments.

Patient	**AARE (degrees)**	**AATE (mm)**
1	0.24	0.03*1.8
2	0.23	0.03*1.8
3	0.42	0.03*1.8
4	0.17	0*1.8
5	0.18	0*1.8
6	0.35	0*1.8
7	0.21	0*1.8
8	0.2	0*1.8
9	0.26	0.03*1.8
10	0.18	0.03*1.8
Average	**0.24**	**0.02*1.8**

Table 12: Average Absolute Rotational and Translational Errors per patient for "10 displacement" T1-T2 registration experiments.

Patient	**AARE (degrees)**	**AATE (mm)**
1	0.36	0.2*1.8
2	0.24	0.2*1.8
3	0.46	0.13*1.8
4	0.27	0.13*1.8
5	0.37	0.03*1.8
6	0.45	0.23*1.8
7	0.32	0.33*1.8
8	0.44	0.03*1.8
9	0.23	0.13*1.8
10	0.49	0.53*1.8
Average	**0.36**	**0.2*1.8**

0.03 to 0.53 voxels). It can be seen that no significant loss in accuracy is measured when going from T1-T1 to T1-T2 registration. This result shows, once more, that our method is surface based. Tables 13 and 14 show the same results as they are computed per geometric transformation and for all patients. It can be seen that the initial misalignment imposed does not affect the registration accuracy of the method.

3.8 3D results - "different times" experiments

In addition to the "10 displacement" experiments, 40 "different times" registration experiments were performed. These experiments were T1-T1 or T1-T2 and aimed at:

a) investigating the surface matching nature of the method

b) identifying the effect of different imaging resolutions to the registration algorithm.

The main results obtained from these experiments will be presented in the next sections.

3.8.1 Half resolution "different times" experiments

The half resolution "different times" experiments were performed to identify changes in the behavior of the registration algorithm between T1-T1 and T1-T2 registration. This was done by measuring the differences in the adjustment values computed by the algorithm for each iteration. The results from these measurements are shown in tables 15 to 18. Table 15 shows the final adjustments per patient for the 10 "half resolution" T1-T1 "different times" experiments. Table 16 shows the same result for the T1-T2 experiments and table 17 shows the absolute differences in the adjustment values of the two previous tables. The differences in rotational parameters vary

Table 13: Average Absolute Rotational and Translational Errors per transformation for "10 displacement" T1-T1 registration experiments.

Transformation	**AARE (degrees)**	**AATE (mm)**
1	0.22	0*1.8
2	0.19	0.03*1.8
3	0.2	0*1.8
4	0.32	0.1*1.8
5	0.32	0.03*1.8
6	0.27	0*1.8
7	0.22	0*1.8
8	0.24	0*1.8
9	0.27	0*1.8
10	0.2	0*1.8
Average	**0.24**	**0.02*1.8**

Table 14: Average Absolute Rotational and Translational Errors per transformation for "10 displacement" T1-T2 registration experiments.

Transformation	**AARE (degrees)**	**AATE (mm)**
1	0.29	0.13*1.8
2	0.3	0.3*1.8
3	0.47	0.13*1.8
4	0.41	0.2*1.8
5	0.48	0.2*1.8
6	0.3	0.17*1.8
7	0.38	0.17*1.8
8	0.34	0.2*1.8
9	0.32	0.23*1.8
10	0.35	0.17*1.8
Average	**0.36**	**0.2*1.8**

Table 15: Final adjustment values per patient for half resolution "different times" T1-T1 registration experiments.

Patient number	**xy rotation (degrees)**	**yz rotation (degrees)**	**zx rotation (degrees)**	**x translation (mm)**	**y translation (mm)**	**z translation (mm)**
1	-2.36	-1.7	-0.33	-4*1.8	-4*1.8	0*1.8
2	5.96	-0.67	1.3	3*1.8	1*1.8	0*1.8
3	-2.92	-1.57	-0.22	-1*1.8	0*1.8	0*1.8
4	-1.91	-0.33	-0.22	-1*1.8	-2*1.8	0*1.8
5	-4.61	0.33	1.12	-2*1.8	0*1.8	-1*1.8
6	2.02	-0.67	0	-15*1.8	-2*1.8	-1*1.8
7	-10.01	0.45	-0.45	-2*1.8	2*1.8	-1*1.8
8	-5.73	-1.68	0	5*1.8	8*1.8	0*1.8
9	0.45	0.11	0.11	-1*1.8	0*1.8	0*1.8
10	-4.61	0.33	0.11	0*1.8	0*1.8	0*1.8

Table 16: Final adjustment values per patient for half resolution "different times" T1-T2 registration experiments.

Patient number	**xy rotation (degrees)**	**yz rotation (degrees)**	**zx rotation (degrees)**	**x translation (mm)**	**y translation (mm)**	**z translation (mm)**
1	-1.91	-1.68	-0.11	-4*1.8	-4*1.8	0*1.8
2	5.96	-0.33	1.12	2*1.8	1*1.8	-1*1.8
3	-2.58	-1.91	-0.22	-1*1.8	-1*1.8	1*1.8
4	-2.02	0.45	-0.33	-1*1.8	-1*1.8	0*1.8
5	-4.38	0	1.25	-2*1.8	-1*1.8	0*1.8
6	1.79	-0.78	-1.57	-14*1.8	-3*1.8	-2*1.8
7	-10.23	0.45	-0.78	-3*1.8	1*1.8	-1*1.8
8	-5.96	-1.12	-0.22	4*1.8	8*1.8	0*1.8
9	0.33	1.12	0.33	-1*1.8	0*1.8	0*1.8
10	-5.51	0.67	0.45	0*1.8	0*1.8	0*1.8

Table 17: Absolute differences of the adjustment values of tables 15 and 16

Patient number	xy rotation (degrees)	yz rotation (degrees)	zx rotation (degrees)	x translation (mm)	y translation (mm)	z translation (mm)
1	0.45	0.02	0.22	0*1.8	0*1.8	0*1.8
2	0	0.34	0.18	1*1.8	0*1.8	1*1.8
3	0.34	0.34	0	0*1.8	1*1.8	1*1.8
4	0.11	0.12	0.11	0*1.8	1*1.8	0*1.8
5	0.23	0.33	0.13	0*1.8	1*1.8	1*1.8
6	0.23	0.11	1.57	1*1.8	1*1.8	1*1.8
7	0.22	0	0.33	1*1.8	1*1.8	0*1.8
8	0.23	0.56	0.22	1*1.8	0*1.8	0*1.8
9	0.12	1.01	0.22	0*1.8	0*1.8	0*1.8
10	0.9	0.34	0.34	0*1.8	0*1.8	0*1.8
Average	0.28	0.32	0.33	0.4*1.8	0.5*1.8	0.4*1.8

Table 18: Absolute differences of adjustment values per iteration for patient 3 between T1-T1 and T1-T2 half resolution "different times" registration experiments

Iteration number	**xy rotation (degrees)**	**yz rotation (degrees)**	**zx rotation (degrees)**	**x translation (mm)**	**y translation (mm)**	**z translation (mm)**
1-6	0.34	0.23	0.11	0*1.8	1*1.8	0*1.8
7-12	0	0.22	0	1*1.8	1*1.8	1*1.8
13-18	0	0.34	0	0*1.8	1*1.8	0*1.8
19-24	0.34	0.34	0	0*1.8	1*1.8	1*1.8
Average	0.17	0.28	0.03	0.25*1.8	1*1.8	0.5*1.8

between 0 and 1.57 degrees with average values 0.28 degrees for xy rotation, 0.32 degrees for yz rotation and 0.33 degrees for zx rotation. The differences in translational parameters vary between 0 and 1 voxel with average values of 0.4 voxels for x translation, 0.5 voxels for y translation and 0.4 voxels for z translation. Table 18 shows the absolute differences in the adjustment values per iteration for the worst-case patient 3. The same trend can be seen, since the rotational adjustment differences are less than 0.34 degrees and the translational adjustment differences are less than 1 voxel. Both of these results show clearly that the performance of the method is not affected by the differences in signal intensity and therefore the method can be considered as surface based.

3.8.2 Full resolution "different times" experiments

The same experiments outlined in the previous section were performed again at full resolution and the results were compared to the results at half resolution. The purpose was to identify the effect of different imaging resolutions on the registration algorithm. Table 19 shows the absolute differences in the final adjustment values between half and full resolution for each patient for T1-T1 registration, and table 20 shows the same result for T1-T2 registration. The average rotational differences are below 0.51 degrees. Tables 21 and 22 show the absolute differences in the adjustment values for each iteration for the worst-case patient. The average rotational differences are less than 0.64 degrees. Translational differences are higher because of the reduced effect of quantization for higher imaging resolutions. Based on these results, it can be shown that

a resolution of 1.8 mm/voxel is sufficient for the registration method and that higher resolution does not seem to improve the registration accuracy.

Table 19: Absolute differences of the final adjustment values per patient between full and half resolution "different times" T1-T1 registration experiments.

Patient	**xy rotation (degrees)**	**yz rotation (degrees)**	**zx rotation (degrees)**	**x translation (mm)**	**y translation (mm)**	**z translation (mm)**
1	0.45	0.77	0.22	0*0.9	1*0.9	0*0.9
2	0.11	0.67	0.1	1*0.9	1*0.9	0*0.9
3	1.24	0.11	0.11	0*0.9	0*0.9	0*0.9
4	0.11	0.66	0.56	0*1.9	2*0.9	1*0.9
5	0.23	0.66	0.8	2*0.9	1*0.9	0*0.9
6	0.9	0	1.12	1*0.9	0*0.9	0*0.9
7	0.34	0.12	0.11	1*0.9	1*0.9	1*0.9
8	0.66	0	0.9	2*0.9	1*0.9	1*0.9
9	0.78	0.11	0.45	1*0.9	1*0.9	2*0.9
10	0.11	0.12	0.11	0*0.9	1*0.9	2*0.9
Average	0.49	0.32	0.45	0.8*0.9	0.9*0.9	0.7*0.9

Table 20: Absolute differences of the final adjustment values per patient between full and half resolution "different times" T1-T2 registration experiments.

Patient number	**xy rotation (degrees)**	**yz rotation (degrees)**	**zx rotation (degrees)**	**x translation (mm)**	**y translation (mm)**	**z translation (mm)**
1	0.45	0.34	0.11	0*0.9	2*0.9	0*0.9
2	0.11	0.22	0.45	1*0.9	1*0.9	2*0.9
3	0.12	0.45	0	0*0.9	1*0.9	1*0.9
4	0.23	0.78	0.23	1*0.9	0*0.9	2*0.9
5	0	0.56	0.56	1*0.9	1*0.9	2*0.9
6	0.79	0.78	0.9	0*0.9	1*0.9	1*0.9
7	0.34	0.12	0.12	0*0.9	1*0.9	1*0.9
8	0.56	0.68	0.22	0*0.9	2*0.9	1*0.9
9	0.11	0.67	0.11	1*0.9	1*0.9	1*0.9
10	0.56	0.45	0.23	0*0.9	2*0.9	1*0.9
Average	0.33	0.51	0.3	0.4*0.9	1.2*0.9	1.2*0.9

Table 21: Absolute differences in adjustment values per iteration for patient 3 between full and half resolution "different times" T1-T1 registration experiments.

Iteration number	xy rotation (degrees)	yz rotation (degrees)	zx rotation (degrees)	x translation (mm)	y translation (mm)	z translation (mm)
1-6	0.1	0.1	0.11	0*0.9	1*0.9	1*0.9
7-12	0.34	0.34	0.11	1*0.9	0*0.9	1*0.9
13-18	0.9	0.11	0.11	0*0.9	1*0.9	0*0.9
19-24	1.24	0.11	0.11	0*0.9	0*0.9	1*0.9
Average	0.64	0.17	0.11	0.25*0.9	0.5*0.9	0.75*0.9

Table 22: Absolute differences in adjustment values per iteration for patient 3 between full and half resolution "different times" T1-T2 registration experiments.

Iteration number	xy rotation (degrees)	yz rotation (degrees)	zx rotation (degrees)	x translation (mm)	y translation (mm)	z translation (mm)
1-6	0.12	0	0.34	0*0.9	0*0.9	0*0.9
7-12	0.11	0.56	0	1*0.9	1*0.9	1*0.9
13-18	0.12	0.45	0	0*0.9	1*0.9	0*0.9
19-24	0.12	0.45	0	0*0.9	1*0.9	1*0.9
Average	0.12	0.37	0.09	0.25*0.9	0.75*0.9	0.5*0.9

1.8 mm/voxel is sufficient for the registration method and that higher resolution does not seem to improve the registration accuracy.

Figures 13 to 14 illustrate the "different times" T1-T1 experiment for patient 7. The T1 image volume of the first imaging date is used as the reference for this experiment. The surface renderings of the volumes appear in figure 13. Figure 14 shows the scans 4, 10, and 16 of the corresponding MR study.

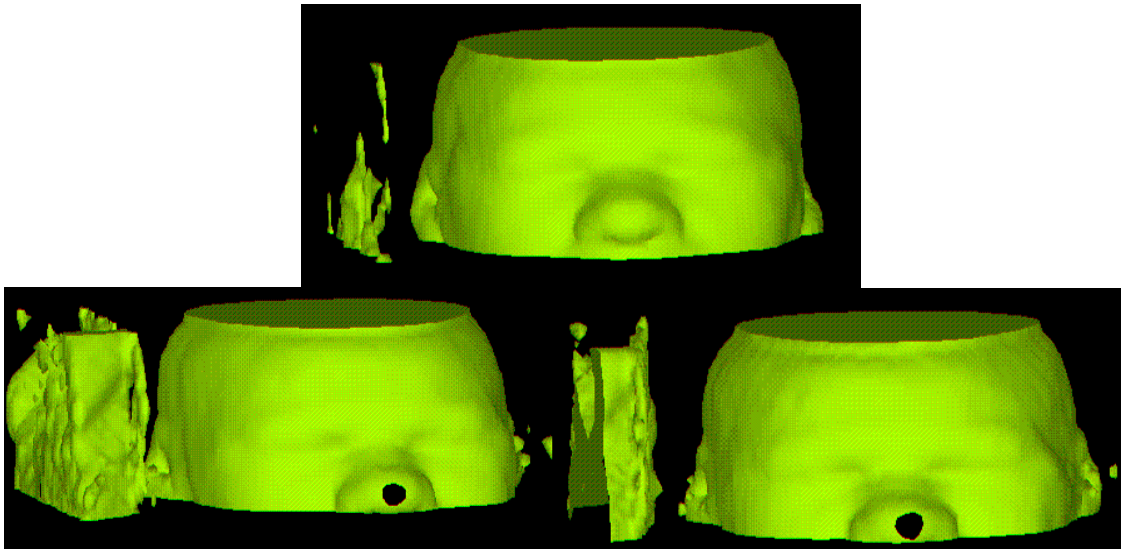

Figure 13: T1-T1 "different times" registration experiments example. Top: Reference T1 volume. Bottom left: Reslice T1 volume before registration. Bottom right: Reslice T1 volume after registration.

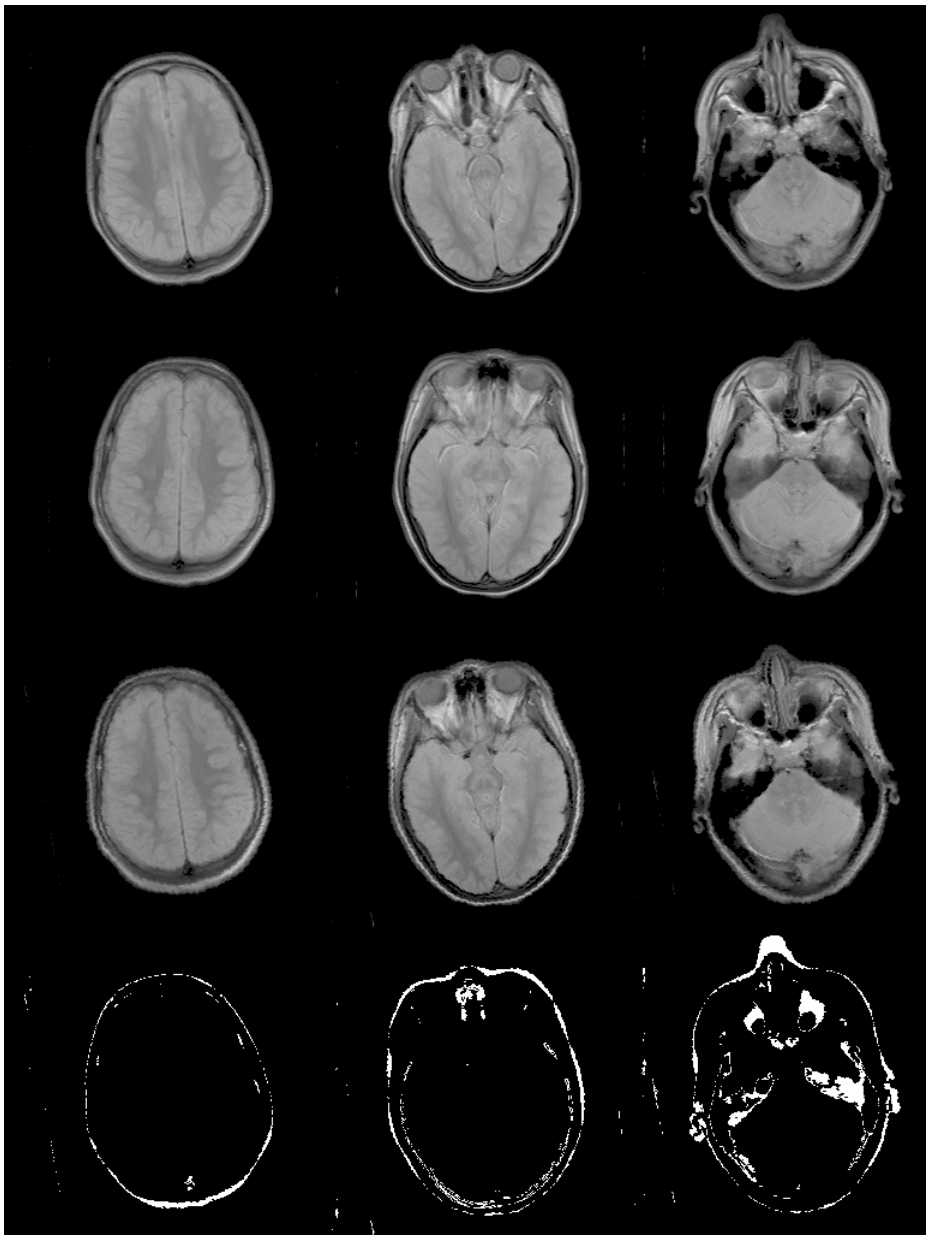

Figure 14: Illustration of the "different times" T1-T1 three-dimensional registration experiments. First row: Scans # 4, 10, 16 of reference image study. Second row: Scans # 4, 10, 16 of reslice image study before registration. Third row: Scans # 4, 10, 16 of reslice image study after registration. Fourth row: White areas show the areas of mismatch between the studies of rows 1 and 3.

CHAPTER IV

EVALUATION OF THE METHOD

4.1 Introduction

Using the results presented in Chapter III, conclusions regarding the accuracy and the surface matching nature of the method and the effect of imaging resolution will be drawn in this chapter. Additionally to the evaluation of the previous chapter's results some more measurements that refer to the effect of non-overlapping segments in the two volumes will be presented. Finally, the ability of the method in its current form to perform non-rigid body registration will be discussed.

4.2 Evaluation of accuracy and surface matching nature of the method

As presented in the previous chapter, the accuracy of the method for T1-T1 and T1-T2 MR image three-dimensional registration was evaluated using the "10 displacement" technique that gave rotational and translational errors less than 1 degree and 1 voxel.

The following cautionary remarks should be noted:

a) The translational error computed by the "10 displacement" method is affected by the quantization effect due to the nearest integer implementation of the geometric transformations. The result of this effect on the error cannot be accurately estimated. The error can be corrected with the incorporation of the trilinear interpolation routine in the geometric transformations routine.

b) Both rotational and translational error estimates for the "10 displacement" technique are acquired under ideal conditions, since the rotated and translated volumes have exactly the same signal areas with the reference ones-something that can never occur in real-life experiments. Some measurements that refer to the effect of non-overlapping segments on the accuracy of the method will be presented later in this chapter.

Safer conclusions can be drawn regarding the surface matching nature of the method. Several results in the previous chapter showed that the behavior of the method is not affected by the differences in signal intensities in the two volumes. When going from T1-T1 to T1-T2 "different times" experiments, the final adjustment values and the adjustments with each iteration do not change significantly. The same holds for the errors as computed with the "10 displacement" technique: these do not deteriorate when studies of different signal intensities are registered. This result shows also either the suitability of the fuzzy c-means for surface definition with MR data or the insensitivity of the method to noise and minor surface differences. Additional studies regarding the effect of noise on the performance of the method are needed.

4.3 Effect of resolution

Deterioration in the imaging resolution was not found to affect significantly the performance of the method as measured by the rotational errors. More studies with the use of floating point operations for translations and also with volumes with voxel size of 3.6 mm should be made to investigate the extent of this effect. The ability of the method to perform well at lower resolutions is an important feature because it increases the speed of the registration procedure.

4.4 Non-overlapping segments

The "10 displacement" experiments were performed under ideal conditions, given that the two volumes had exactly the same signal area. To investigate the effect of non-overlapping segments on the accuracy of the method, experiments with volumes from different parts of the head were performed. These experiments used the T1 and T2 data from the first imaging date of patient 1 and geometric transformation 1. The presence of non-overlapping segments along the z dimension was assured by using scans 1-10 for the T1 study and scans (1+i) - (10+i) for the T2 study with i=0...9. All the experiments were performed at half resolution using a voxel size of 1.8 mm. The number of the experiment and the scans used for each study appear in table 23. The errors computed for each experiment and for each transformation parameter are shown in table 24. Although this

Table 23: Numbers of scans from each study used for the 10 non-overlapping segment experiments.

Experiment	**T1 study scans**	**T2 study scans**
1	1-10	1-10
2	1-10	2-11
3	1-10	3-12
4	1-10	4-13
5	1-10	5-14
6	1-10	6-15
7	1-10	7-16
8	1-10	8-17
9	1-10	9-18
10	1-10	10-19

Table 24: Final adjustment errors per transformation parameter for the non-overlapping segment experiments.

Exper #	**xy rot (degrees)**	**yz rot (degrees)**	**zx rot (degrees)**	**x trans (voxels)**	**y trans (voxels)**	**z trans (voxels)**
1	-1.03	0.14	-0.86	1	-1	-1
2	-0.69	0.65	-0.41	0	0	1
3	-1.59	0.93	-0.18	0	1	1
4	-3.39	0.59	-0.07	0	0	1
5	-5.08	-0.19	0.38	0	1	1
6	-6.77	-0.3	-0.52	0	1	1
7	-7.22	-0.07	-0.52	0	1	1
8	-7.78	-0.64	-0.07	0	2	1
9	-7.33	-0.3	0.71	0	2	2
10	-6.99	-0.3	0.48	0	3	2

result is preliminary and further analysis of the effect of non-overlapping segments effect is needed, the following two points are of interest:

a) The presence of non-overlapping segments along the z dimension affects the z-translation error, which stays constant and close to zero, whereas it should follow the increase in the extent of the non-overlapping segments. The presence of non-overlapping segments also increases the xy plane rotation error for areas of non-overlap more than 3 layers of non-cubic voxels. No effect on the x and y translation errors seems to exist.

b) Non-overlapping segments along the z axis did not affect yz, zx plane rotations. This result could be attributed to the fact that the rotation of the reslice volume is artificial and is performed after the interpolation, whereas in a real experiment, slicing and interpolation along the z axis are performed after the rotations.

More studies are needed to investigate whether the above observations are correct.

4.5 Non-rigid body registration

Another aspect of our method that needs to be investigated is how well it can perform non-rigid body registration. For three-dimensional registration in the presence of linear or non-linear scaling in the two volumes, the following points are interesting:

a) The registration function gets its minimum value for the correct registration position.

b) The iteration loop with the use of the symmetry of the Chebyshev points is not appropriate for minimizing this function. An iteration loop that treats linear scaling as three more geometric transformations will de-register and scale two non-scaled and registered volumes. Additional changes to the algorithm will need to address how to compute the minimum of the registration function for non-rigid body registration. This area is open for future investigation.

APPENDIX A

PATIENT DATA AND RESULTS

Table 25: Examination data for the 10 patients

Patient Number	1st Exam. Date	2nd Exam Date	Disease
1	Oct 10, 94	Feb 6, 95	Meningioma
2	Nov 7, 94	Nov 16, 94	Encephalitis
3	Nov 3, 94	Dec 21, 94	Encephalitis
4	Jul 20, 94	Oct 12, 94	Unknown
5	Aug 9, 94	Feb 12, 95	Epilepsy
6	Oct 22, 94	Jan 3, 95	Leukemia
7	Nov 4, 94	Feb 2, 95	Epilepsy
8	Dec 3, 94	Jan 19, 95	Glioblastoma
9	Oct 12, 94	Feb 22, 95	Glioblastoma
10	Dec 12, 94	Jan 13, 95	Astrocytoma

Table 26: Final adjustment errors per patient for all the T1-T1 "10 displacement" 3D registration experiments.

Patient #	Trans #	xy rot	yz rot	zx rot	x trans	y trans	z trans
1	**1**	**0.09**	**-0.1**	**0.03**	**0**	**0**	**0**
1	**2**	**-0.4**	**0.29**	**-0.1**	**0**	**0**	**0**
1	**3**	**0.08**	**0.01**	**0.1**	**0**	**0**	**0**
1	**4**	**0.36**	**-0.9**	**0.11**	**0**	**-1**	**0**
1	**5**	**0.08**	**0.22**	**-0.13**	**0**	**0**	**0**
1	**6**	**0.47**	**-0.37**	**0.27**	**0**	**0**	**0**
1	**7**	**0.36**	**0.16**	**-0.12**	**0**	**0**	**0**
1	**8**	**0.36**	**-0.18**	**-0.21**	**0**	**0**	**0**
1	**9**	**-0.47**	**0.48**	**-0.26**	**0**	**0**	**0**
1	**10**	**-0.01**	**0.47**	**-0.06**	**0**	**0**	**0**
1	**Average**	**0.27**	**0.32**	**0.14**	**0**	**0.1**	**0**
2	1	-0.13	0.41	0.04	0	0	0
2	2	-0.29	0.07	0.35	0	0	0
2	3	0.42	0.3	-0.23	0	0	0
2	4	0.24	-0.22	0.55	1	0	0
2	5	-0.25	0	0.55	0	0	0
2	6	0.36	-0.26	-0.06	0	0	0
2	7	0.14	-0.4	-0.23	0	0	0
2	8	-0.09	0.15	-0.04	0	0	0
2	9	0.09	-0.41	0.37	0	0	0
2	10	-0.01	-0.03	-0.07	0	0	0
2	Average	0.2	0.23	0.25	0.1	0	0
3	**1**	**-0.24**	**-0.52**	**-0.41**	**0**	**0**	**0**
3	**2**	**0.6**	**-0.15**	**-0.43**	**0**	**0**	**0**
3	**3**	**-0.48**	**0.06**	**0.1**	**0**	**0**	**0**
3	**4**	**1.03**	**-0.78**	**0.23**	**0**	**0**	**0**
3	**5**	**-2.1**	**-0.11**	**-0.69**	**1**	**0**	**0**
3	**6**	**0.13**	**-0.48**	**-0.62**	**0**	**0**	**0**
3	**7**	**-0.42**	**-0.17**	**0.21**	**0**	**0**	**0**
3	**8**	**-0.2**	**0.02**	**-0.1**	**0**	**0**	**0**
3	**9**	**-0.36**	**0.59**	**0.19**	**0**	**0**	**0**
3	**10**	**-0.01**	**-0.31**	**-0.73**	**0**	**0**	**0**
3	**Average**	**0.56**	**0.32**	**0.37**	**0.1**	**0**	**0**
4	1	0.09	-0.07	0.03	0	0	0
4	2	-0.06	0.07	-0.32	0	0	0

Table 26 (Continued)

4	3	-0.03	-0.1	0.21	0	0	0
4	4	-0.31	-0.04	-0.1	0	0	0
4	5	0.42	-0.33	-0.02	0	0	0
4	6	-0.09	0.18	-0.06	0	0	0
4	7	0.25	-0.39	-0.01	0	0	0
4	8	-0.09	-0.3	-0.21	0	0	0
4	9	0.42	-0.41	-0.03	0	0	0
4	10	0.21	0.08	0.05	0	0	0
4	Average	0.2	0.2	0.1	0	0	0
5	**1**	**0.09**	**-0.19**	**0.26**	**0**	**0**	**0**
5	**2**	**-0.18**	**-0.04**	**-0.21**	**0**	**0**	**0**
5	**3**	**0.08**	**0.12**	**0.1**	**0**	**0**	**0**
5	**4**	**-0.2**	**-0.45**	**-0.21**	**0**	**0**	**0**
5	**5**	**-0.14**	**-0.22**	**-0.24**	**0**	**0**	**0**
5	**6**	**0.36**	**-0.03**	**0.27**	**0**	**0**	**0**
5	**7**	**0.36**	**-0.18**	**-0.01**	**0**	**0**	**0**
5	**8**	**-0.54**	**-0.02**	**-0.1**	**0**	**0**	**0**
5	**9**	**-0.24**	**-0.41**	**-0.03**	**0**	**0**	**0**
5	**10**	**0.15**	**0.03**	**-0.07**	**0**	**0**	**0**
5	**Average**	**0.23**	**0.17**	**0.15**	**0**	**0**	**0**
6	1	-0.24	-0.3	0.6	0	0	0
6	2	-0.18	-0.38	-0.1	0	0	0
6	3	-0.93	0.45	0.66	0	0	0
6	4	0.24	0.11	-0.21	0	0	0
6	5	0.02	-0.33	0.65	0	0	0
6	6	-0.09	0.52	0.05	0	0	0
6	7	0.14	-0.06	0.55	0	0	0
6	8	0.24	-0.3	0.57	0	0	0
6	9	0.31	0.14	0.64	0	0	0
6	10	-0.57	0.36	-0.4	0	0	0
6	Average	0.3	0.3	0.44	0	0	0
7	**1**	**-0.47**	**-0.13**	**0.26**	**0**	**0**	**0**
7	**2**	**-0.18**	**-0.19**	**0.01**	**0**	**0**	**0**
7	**3**	**0.08**	**0.12**	**-0.01**	**0**	**0**	**0**
7	**4**	**-0.2**	**-0.22**	**0.46**	**0**	**0**	**0**
7	**5**	**-0.25**	**-0.33**	**-0.24**	**0**	**0**	**0**
7	**6**	**-0.2**	**0.29**	**0.27**	**0**	**0**	**0**
7	**7**	**0.03**	**0.05**	**-0.35**	**0**	**0**	**0**
7	**8**	**-0.09**	**0.04**	**-0.66**	**0**	**0**	**0**
7	**9**	**-0.36**	**-0.3**	**0.07**	**0**	**0**	**0**

Table 26 (Continued)

7	**10**	**0.21**	**0.03**	**-0.12**	**0**	**0**	**0**
7	**Average**	**0.21**	**0.17**	**0.25**	**0**	**0**	**0**
8	1	-0.02	-0.19	-0.18	0	0	0
8	2	-0.18	0.07	-0.21	0	0	0
8	3	-0.03	0.12	0.21	0	0	0
8	4	-0.31	0.11	-0.21	0	0	0
8	5	-0.14	0.11	0.53	0	0	0
8	6	0.24	-0.03	-0.17	0	0	0
8	7	0.03	0.61	0.32	0	0	0
8	8	-0.2	0.26	-0.21	0	0	0
8	9	0.31	-0.07	-0.26	0	0	0
8	10	-0.01	-0.53	0.05	0	0	0
8	Average	0.15	0.21	0.24	0	0	0
9	**1**	**-0.13**	**0.48**	**0.15**	**0**	**0**	**0**
9	**2**	**-0.29**	**-0.26**	**0.06**	**0**	**0**	**0**
9	**3**	**-0.36**	**0.01**	**-0.12**	**0**	**0**	**0**
9	**4**	**0.69**	**-0.67**	**0.12**	**0**	**-1**	**0**
9	**5**	**-0.48**	**0.45**	**-0.24**	**0**	**0**	**0**
9	**6**	**-0.09**	**0.3**	**-0.06**	**0**	**0**	**0**
9	**7**	**-0.08**	**0.5**	**0.1**	**0**	**0**	**0**
9	**8**	**0.36**	**0.26**	**-0.55**	**0**	**0**	**0**
9	**9**	**-0.13**	**-0.02**	**-0.03**	**0**	**0**	**0**
9	**10**	**-0.01**	**-0.53**	**-0.17**	**0**	**0**	**0**
9	**Average**	**0.26**	**0.35**	**0.16**	**0**	**0.1**	**0**
10	1	-0.02	-0.3	0.37	0	0	0
10	2	0.04	0.01	0.01	1	0	0
10	3	-0.25	0.12	0.1	0	0	0
10	4	0.02	-0.22	-0.04	0	0	0
10	5	-0.14	0	-0.13	0	0	0
10	6	0.58	-0.6	0.05	0	0	0
10	7	-0.19	0.16	-0.12	0	0	0
10	8	-0.2	0.15	0.23	0	0	0
10	9	-0.02	0.48	0.07	0	0	0
10	10	-0.01	0.47	0.27	0	0	0
10	Average	0.15	0.25	0.14	0.1	0	0

Table 27: Final adjustment errors per geometric transformation for all the T1-T1 "10 displacement" 3D registration experiments.

Trans #	Patient #	xy rot	yz rot	zx rot	x trans	y trans	z trans
1	**1**	**0.09**	**-0.1**	**0.03**	**0**	**0**	**0**
1	**2**	**-0.13**	**0.41**	**0.04**	**0**	**0**	**0**
1	**3**	**-0.24**	**-0.52**	**-0.41**	**0**	**0**	**0**
1	**4**	**0.09**	**-0.07**	**0.03**	**0**	**0**	**0**
1	**5**	**0.09**	**-0.19**	**0.26**	**0**	**0**	**0**
1	**6**	**-0.24**	**-0.3**	**0.6**	**0**	**0**	**0**
1	**7**	**-0.47**	**-0.13**	**0.26**	**0**	**0**	**0**
1	**8**	**-0.02**	**-0.19**	**-0.18**	**0**	**0**	**0**
1	**9**	**-0.13**	**0.48**	**0.15**	**0**	**0**	**0**
1	**10**	**-0.02**	**-0.3**	**0.37**	**0**	**0**	**0**
1	**Average**	**0.15**	**0.27**	**0.23**	**0**	**0**	**0**
2	1	-0.4	0.29	-0.1	0	0	0
2	2	-0.29	0.07	0.35	0	0	0
2	3	0.6	-0.15	-0.43	0	0	0
2	4	-0.06	0.07	-0.32	0	0	0
2	5	-0.18	-0.04	-0.21	0	0	0
2	6	-0.18	-0.38	-0.1	0	0	0
2	7	-0.18	-0.19	0.01	0	0	0
2	8	-0.18	0.07	-0.21	0	0	0
2	9	-0.29	-0.26	0.06	0	0	0
2	10	0.04	0.01	0.01	1	0	0
2	Average	0.24	0.15	0.18	0.1	0	0
3	**1**	**0.08**	**0.01**	**0.1**	**0**	**0**	**0**
3	**2**	**0.42**	**0.3**	**-0.23**	**0**	**0**	**0**
3	**3**	**-0.48**	**0.06**	**0.1**	**0**	**0**	**0**
3	**4**	**-0.03**	**-0.1**	**0.21**	**0**	**0**	**0**
3	**5**	**0.08**	**0.12**	**0.1**	**0**	**0**	**0**
3	**6**	**-0.93**	**0.45**	**0.66**	**0**	**0**	**0**
3	**7**	**0.08**	**0.12**	**-0.01**	**0**	**0**	**0**
3	**8**	**-0.03**	**0.12**	**0.21**	**0**	**0**	**0**
3	**9**	**-0.36**	**0.01**	**-0.12**	**0**	**0**	**0**
3	**10**	**-0.25**	**0.12**	**0.1**	**0**	**0**	**0**
3	**Average**	**0.27**	**0.14**	**0.18**	**0**	**0**	**0**
4	1	0.36	-0.9	0.11	0	-1	0
4	2	0.24	-0.22	0.55	1	0	0
4	3	1.03	-0.78	0.23	0	0	0
4	4	-0.31	-0.04	-0.1	0	0	0

Table 27 (Continued)

4	5	-0.2	-0.45	-0.21	0	0	0
4	6	0.24	0.11	-0.21	0	0	0
4	7	-0.2	-0.22	0.46	0	0	0
4	8	-0.31	0.11	-0.21	0	0	0
4	9	0.69	-0.67	0.12	0	-1	0
4	10	0.02	-0.22	-0.04	0	0	0
4	Average	0.36	0.37	0.22	0.1	0.2	0
5	**1**	**0.08**	**0.22**	**-0.13**	**0**	**0**	**0**
5	**2**	**-0.25**	**0**	**0.55**	**0**	**0**	**0**
5	**3**	**-2.1**	**-0.11**	**-0.69**	**1**	**0**	**0**
5	**4**	**0.42**	**-0.33**	**-0.02**	**0**	**0**	**0**
5	**5**	**-0.14**	**-0.22**	**-0.24**	**0**	**0**	**0**
5	**6**	**0.02**	**-0.33**	**0.65**	**0**	**0**	**0**
5	**7**	**-0.25**	**-0.33**	**-0.24**	**0**	**0**	**0**
5	**8**	**-0.14**	**0.11**	**0.53**	**0**	**0**	**0**
5	**9**	**-0.48**	**0.45**	**-0.24**	**0**	**0**	**0**
5	**10**	**-0.14**	**0**	**-0.13**	**0**	**0**	**0**
5	**Average**	**0.4**	**0.21**	**0.34**	**0.1**	**0**	**0**
6	1	0.47	-0.37	0.27	0	0	0
6	2	0.36	-0.26	-0.06	0	0	0
6	3	0.13	-0.48	-0.62	0	0	0
6	4	-0.09	0.18	-0.06	0	0	0
6	5	0.36	-0.03	0.27	0	0	0
6	6	-0.09	0.52	0.05	0	0	0
6	7	-0.2	0.29	0.27	0	0	0
6	8	0.24	-0.03	-0.17	0	0	0
6	9	-0.09	0.3	-0.06	0	0	0
6	10	0.58	-0.6	0.05	0	0	0
6	Average	0.31	0.31	0.19	0	0	0
7	**1**	**0.36**	**0.16**	**-0.12**	**0**	**0**	**0**
7	**2**	**0.14**	**-0.4**	**-0.23**	**0**	**0**	**0**
7	**3**	**-0.42**	**-0.17**	**0.21**	**0**	**0**	**0**
7	**4**	**0.25**	**-0.39**	**-0.01**	**0**	**0**	**0**
7	**5**	**0.36**	**-0.18**	**-0.01**	**0**	**0**	**0**
7	**6**	**0.14**	**-0.06**	**0.55**	**0**	**0**	**0**
7	**7**	**0.03**	**0.05**	**-0.35**	**0**	**0**	**0**
7	**8**	**0.03**	**0.61**	**0.32**	**0**	**0**	**0**
7	**9**	**-0.08**	**0.5**	**0.1**	**0**	**0**	**0**
7	**10**	**-0.19**	**0.16**	**-0.12**	**0**	**0**	**0**
7	**Average**	**0.2**	**0.27**	**0.2**	**0**	**0**	**0**

Table 27 (Continued)

8	1	0.36	-0.18	-0.21	0	0	0
8	2	-0.09	0.15	-0.04	0	0	0
8	3	-0.2	0.02	-0.1	0	0	0
8	4	-0.09	-0.3	-0.21	0	0	0
8	5	-0.54	-0.02	-0.1	0	0	0
8	6	0.24	-0.3	0.57	0	0	0
8	7	-0.09	0.04	0.66	0	0	0
8	8	-0.2	0.26	-0.21	0	0	0
8	9	0.36	0.26	-0.55	0	0	0
8	10	-0.2	0.15	0.23	0	0	0
8	Average	0.24	0.19	0.29	0	0	0
9	**1**	**-0.47**	**0.48**	**-0.26**	**0**	**0**	**0**
9	**2**	**0.09**	**-0.41**	**0.37**	**0**	**0**	**0**
9	**3**	**-0.36**	**0.59**	**0.19**	**0**	**0**	**0**
9	**4**	**0.42**	**-0.41**	**-0.03**	**0**	**0**	**0**
9	**5**	**-0.24**	**-0.41**	**-0.03**	**0**	**0**	**0**
9	**6**	**0.31**	**0.14**	**0.64**	**0**	**0**	**0**
9	**7**	**-0.36**	**-0.3**	**0.07**	**0**	**0**	**0**
9	**8**	**0.31**	**-0.07**	**-0.26**	**0**	**0**	**0**
9	**9**	**-0.13**	**-0.02**	**-0.03**	**0**	**0**	**0**
9	**10**	**-0.02**	**0.48**	**0.07**	**0**	**0**	**0**
9	**Average**	**0.27**	**0.33**	**0.2**	**0**	**0**	**0**
10	1	-0.01	0.47	-0.06	0	0	0
10	2	-0.01	-0.03	-0.07	0	0	0
10	3	-0.01	-0.31	-0.73	0	0	0
10	4	0.21	0.08	0.05	0	0	0
10	5	0.15	0.03	-0.07	0	0	0
10	6	-0.57	0.36	-0.4	0	0	0
10	7	0.21	0.03	-0.12	0	0	0
10	8	-0.01	-0.53	0.05	0	0	0
10	9	-0.01	-0.53	-0.17	0	0	0
10	10	-0.01	0.47	0.27	0	0	0
10	Average	0.12	0.28	0.2	0	0	0

Table 28: Final adjustment errors per patient for all the T1-T2 "10 displacement" 3D registration experiments.

Patient #	Trans #	xy rot	yz rot	zx rot	x trans	y trans	z trans
1	**1**	**0.09**	**0.48**	**0.03**	**0**	**0**	**0**
1	**2**	**-0.06**	**0.52**	**0.23**	**0**	**-1**	**1**
1	**3**	**-0.25**	**-0.68**	**-0.12**	**0**	**0**	**0**
1	**4**	**0.47**	**1.35**	**0.01**	**0**	**0**	**0**
1	**5**	**-0.25**	**0.78**	**0.65**	**0**	**0**	**1**
1	**6**	**0.02**	**-0.48**	**0.05**	**0**	**-1**	**0**
1	**7**	**0.36**	**0.61**	**-0.35**	**0**	**0**	**0**
1	**8**	**0.13**	**0.49**	**-0.1**	**0**	**0**	**0**
1	**9**	**0.2**	**1.1**	**-0.03**	**0**	**0**	**0**
1	**10**	**0.54**	**-0.19**	**-0.17**	**0**	**-1**	**1**
1	**Average**	**0.24**	**0.67**	**0.17**	**0**	**0.3**	**0.3**
2	1	0.31	0.53	-0.07	0	0	0
2	2	-0.29	-0.04	0.23	0	-1	0
2	3	-0.48	0.57	-0.23	0	0	0
2	4	-0.42	-0.33	-0.1	0	-1	0
2	5	-0.03	1.01	-0.24	0	0	0
2	6	0.02	0.18	-0.28	0	0	0
2	7	0.03	0.05	0.21	0	-1	0
2	8	-0.2	0.04	0.12	0	-1	0
2	9	0.09	0.03	-0.03	0	-1	0
2	10	0.21	0.36	-0.39	0	-1	0
2	Average	0.21	0.31	0.19	0	0.6	0
3	**1**	**-0.36**	**0.03**	**-0.18**	**0**	**0**	**0**
3	**2**	**-0.29**	**-0.6**	**0.23**	**0**	**0**	**0**
3	**3**	**-1.49**	**-0.44**	**0.43**	**0**	**0**	**0**
3	**4**	**0.92**	**-0.45**	**0.57**	**0**	**-1**	**0**
3	**5**	**-1.54**	**-0.78**	**-0.36**	**0**	**-1**	**0**
3	**6**	**0.36**	**0.41**	**-0.06**	**0**	**-1**	**0**
3	**7**	**-0.75**	**-0.39**	**0.32**	**0**	**0**	**0**
3	**8**	**-0.2**	**0.03**	**0.46**	**0**	**0**	**0**
3	**9**	**0.58**	**0.37**	**0.3**	**0**	**-1**	**0**
3	**10**	**-0.24**	**0.25**	**-0.39**	**0**	**0**	**0**
3	**Average**	**0.67**	**0.37**	**0.33**	**0**	**0.4**	**0**
4	1	0.54	0.14	0.15	0	0	0
4	2	-0.07	0.07	0.01	0	1	0
4	3	0.75	-1	0.32	0	-1	0
4	4	-0.09	0.73	0.01	0	1	0

Table 28 (Continued)

4	5	0.53	0.11	0.09	0	0	0
4	6	0.58	0.18	0.05	0	0	0
4	7	0.59	0.11	0.09	0	0	0
4	8	0.58	0.09	0.12	0	1	0
4	9	0.09	-0.41	0.07	0	0	0
4	10	0.21	0.25	-0.06	0	0	0
4	Average	0.4	0.31	0.1	0	0.4	0
5	**1**	**0.09**	**0.09**	**0.26**	**0**	**0**	**0**
5	**2**	**0.27**	**-0.83**	**0.01**	**0**	**-1**	**0**
5	**3**	**0.53**	**0.01**	**0.1**	**0**	**0**	**0**
5	**4**	**-0.54**	**0.62**	**0.12**	**0**	**0**	**0**
5	**5**	**0.08**	**1.01**	**0.42**	**0**	**0**	**0**
5	**6**	**0.36**	**0.86**	**0.27**	**0**	**0**	**0**
5	**7**	**0.36**	**0.5**	**0.21**	**0**	**0**	**0**
5	**8**	**-0.65**	**0.09**	**0.12**	**0**	**0**	**0**
5	**9**	**0.42**	**0.93**	**0.19**	**0**	**0**	**0**
5	**10**	**0.32**	**0.53**	**0.27**	**0**	**0**	**0**
5	**Average**	**0.36**	**0.55**	**0.2**	**0**	**0.1**	**0**
6	1	-0.58	0.14	0.37	0	-1	0
6	2	-0.51	0.18	-0.55	0	-1	0
6	3	-1.15	0.9	0.04	0	0	0
6	4	0.03	-0.11	-0.66	0	-1	0
6	5	-0.64	0.11	1.66	0	-1	0
6	6	0.13	0.3	0.27	0	-1	0
6	7	-0.64	0.05	0.77	0	0	0
6	8	-0.31	0.6	0.68	0	0	0
6	9	-0.31	0.71	0.75	0	-1	0
6	10	-0.18	0.14	-0.17	0	-1	0
6	Average	0.45	0.32	0.59	0	0.7	0
7	**1**	**-0.36**	**0.82**	**-0.07**	**0**	**-1**	**0**
7	**2**	**-0.29**	**0.12**	**-0.1**	**0**	**-1**	**0**
7	**3**	**0.08**	**0.34**	**0.43**	**0**	**-1**	**0**
7	**4**	**0.36**	**0**	**0.01**	**0**	**0**	**0**
7	**5**	**0.3**	**0.11**	**0.76**	**0**	**-1**	**0**
7	**6**	**0.02**	**-0.37**	**-0.28**	**0**	**-1**	**1**
7	**7**	**-0.3**	**0.38**	**-0.35**	**0**	**-1**	**0**
7	**8**	**-0.54**	**0.37**	**-0.66**	**0**	**-1**	**0**
7	**9**	**-0.36**	**0.03**	**0.07**	**0**	**-1**	**1**
7	**10**	**-0.46**	**0.7**	**-0.62**	**0**	**0**	**0**
7	**Average**	**0.31**	**0.32**	**0.34**	**0**	**0.8**	**0.2**

Table 28 (Continued)

8	1	-0.47	0.59	0.03	0	0	0
8	2	-0.63	0.97	0.12	0	0	0
8	3	-0.48	0.34	0.1	0	0	0
8	4	-0.76	1.23	0.12	0	1	0
8	5	-0.03	0.79	-0.24	0	0	0
8	6	-0.09	0.97	0.38	0	0	0
8	7	-0.3	0.5	0.32	0	0	0
8	8	-0.31	0.82	-0.1	0	0	0
8	9	0.09	0.03	0.41	0	0	0
8	10	-0.35	1.26	0.38	0	0	0
8	Average	0.35	0.75	0.22	0	0.1	0
9	**1**	**-0.36**	**0.59**	**-0.18**	**0**	**0**	**0**
9	**2**	**-0.18**	**0.29**	**0.01**	**0**	**0**	**0**
9	**3**	**-0.59**	**0.12**	**-0.01**	**0**	**-1**	**0**
9	**4**	**-0.09**	**-0.11**	**-0.32**	**0**	**0**	**0**
9	**5**	**-0.2**	**0.11**	**-0.02**	**0**	**0**	**0**
9	**6**	**-0.09**	**-0.26**	**-0.06**	**0**	**-1**	**0**
9	**7**	**-0.08**	**0.83**	**-0.23**	**0**	**0**	**0**
9	**8**	**0.13**	**-0.63**	**-0.32**	**0**	**-1**	**0**
9	**9**	**-0.24**	**0.03**	**0.08**	**-1**	**0**	**0**
9	**10**	**-0.01**	**0.47**	**-0.28**	**0**	**0**	**0**
9	**Average**	**0.2**	**0.34**	**0.15**	**0.1**	**0.3**	**0**
10	1	-0.36	0.14	-0.18	0	2	0
10	2	-0.63	-0.15	-0.55	0	2	0
10	3	-1.04	-0.66	0.55	0	1	0
10	4	0.02	-1.12	-0.55	0	1	0
10	5	-0.92	-0.22	0.42	0	1	-1
10	6	-0.42	-0.82	-0.28	0	1	0
10	7	-1.2	-0.51	-0.01	0	2	-1
10	8	-0.99	0.15	0.12	0	2	0
10	9	-0.69	-0.52	0.3	0	1	0
10	10	-0.46	-0.64	-0.06	0	1	0
10	Average	0.67	0.49	0.3	0	1.4	0.2

Table 29: Final adjustment errors per geometric transformation for all the T1-T2 "10 displacement" 3D registration experiments

Trans #	Patient #	xy rot	yz rot	zx rot	x trans	y trans	z trans
1	**1**	**0.09**	**0.48**	**0.03**	**0**	**0**	**0**
1	**2**	**0.31**	**0.53**	**-0.07**	**0**	**0**	**0**
1	**3**	**-0.36**	**0.03**	**-0.18**	**0**	**0**	**0**
1	**4**	**0.54**	**0.14**	**0.15**	**0**	**0**	**0**
1	**5**	**0.09**	**0.09**	**0.26**	**0**	**0**	**0**
1	**6**	**-0.58**	**0.14**	**0.37**	**0**	**-1**	**0**
1	**7**	**-0.36**	**0.82**	**-0.07**	**0**	**-1**	**0**
1	**8**	**-0.47**	**0.59**	**0.03**	**0**	**0**	**0**
1	**9**	**-0.36**	**0.59**	**-0.18**	**0**	**0**	**0**
1	**10**	**-0.36**	**0.14**	**-0.18**	**0**	**2**	**0**
1	**Average**	**0.35**	**0.36**	**0.15**	**0**	**0.4**	**0**
2	1	-0.06	0.52	0.23	0	-1	1
2	2	-0.29	-0.04	0.23	0	-1	0
2	3	-0.29	-0.6	0.23	0	0	0
2	4	-0.07	0.07	0.01	0	1	0
2	5	0.27	-0.83	0.01	0	-1	0
2	6	-0.51	0.18	-0.55	0	-1	0
2	7	-0.29	0.12	-0.1	0	-1	0
2	8	-0.63	0.97	0.12	0	0	0
2	9	-0.18	0.29	0.01	0	0	0
2	10	-0.63	-0.15	-0.55	0	2	0
2	Average	0.32	0.38	0.2	0	0.8	0.1
3	**1**	**-0.25**	**-0.68**	**-0.12**	**0**	**0**	**0**
3	**2**	**-0.48**	**0.57**	**-0.23**	**0**	**0**	**0**
3	**3**	**-1.49**	**-0.44**	**0.43**	**0**	**0**	**0**
3	**4**	**0.75**	**-1**	**0.32**	**0**	**-1**	**0**
3	**5**	**0.53**	**0.01**	**0.1**	**0**	**0**	**0**
3	**6**	**-1.15**	**0.9**	**0.04**	**0**	**0**	**0**
3	**7**	**0.08**	**0.34**	**0.43**	**0**	**-1**	**0**
3	**8**	**-0.48**	**0.34**	**0.1**	**0**	**0**	**0**
3	**9**	**-0.59**	**0.12**	**-0.01**	**0**	**-1**	**0**
3	**10**	**-1.04**	**-0.66**	**0.55**	**0**	**1**	**0**
3	**Average**	**0.68**	**0.51**	**0.23**	**0**	**0.4**	**0**
4	1	0.47	1.35	0.01	0	0	0
4	2	-0.42	-0.33	-0.1	0	-1	0
4	3	0.92	-0.45	0.57	0	-1	0
4	4	-0.09	0.73	0.01	0	1	0

Table 29 (Continued)

4	5	-0.54	0.62	0.12	0	0	0
4	6	0.03	-0.11	-0.66	0	-1	0
4	7	0.36	0	0.01	0	0	0
4	8	-0.76	1.23	0.12	0	1	0
4	9	-0.09	-0.11	-0.32	0	0	0
4	10	0.02	-1.12	-0.55	0	1	0
4	Average	0.37	0.61	0.25	0	0.6	0
5	**1**	**-0.25**	**0.78**	**0.65**	**0**	**0**	**1**
5	**2**	**-0.03**	**1.01**	**-0.24**	**0**	**0**	**0**
5	**3**	**-1.54**	**-0.78**	**-0.36**	**0**	**-1**	**0**
5	**4**	**0.53**	**0.11**	**0.09**	**0**	**0**	**0**
5	**5**	**0.08**	**1.01**	**0.42**	**0**	**0**	**0**
5	**6**	**-0.64**	**0.11**	**1.66**	**0**	**-1**	**0**
5	**7**	**0.3**	**0.11**	**0.76**	**0**	**-1**	**0**
5	**8**	**-0.03**	**0.79**	**-0.24**	**0**	**0**	**0**
5	**9**	**-0.2**	**0.11**	**-0.02**	**0**	**0**	**0**
5	**10**	**-0.92**	**-0.22**	**0.42**	**0**	**1**	**-1**
5	**Average**	**0.45**	**0.5**	**0.49**	**0**	**0.4**	**0.2**
6	1	0.02	-0.48	0.05	0	-1	0
6	2	0.02	0.18	-0.28	0	0	0
6	3	0.36	0.41	-0.06	0	-1	0
6	4	0.58	0.18	0.05	0	0	0
6	5	0.36	0.86	0.27	0	0	0
6	6	0.13	0.3	0.27	0	-1	0
6	7	0.02	-0.37	-0.28	0	-1	1
6	8	-0.09	0.97	0.38	0	0	0
6	9	-0.09	-0.26	-0.06	0	-1	0
6	10	-0.42	-0.82	-0.28	0	1	0
6	Average	0.21	0.48	0.2	0	0.6	0.1
7	**1**	**0.36**	**0.61**	**-0.35**	**0**	**0**	**0**
7	**2**	**0.03**	**0.05**	**0.21**	**0**	**-1**	**0**
7	**3**	**-0.75**	**-0.39**	**0.32**	**0**	**0**	**0**
7	**4**	**0.59**	**0.11**	**0.09**	**0**	**0**	**0**
7	**5**	**0.36**	**0.5**	**0.21**	**0**	**0**	**0**
7	**6**	**-0.64**	**0.05**	**0.77**	**0**	**0**	**0**
7	**7**	**-0.3**	**0.38**	**-0.35**	**0**	**-1**	**0**
7	**8**	**-0.3**	**0.5**	**0.32**	**0**	**0**	**0**
7	**9**	**-0.08**	**0.83**	**-0.23**	**0**	**0**	**0**
7	**10**	**-1.2**	**-0.51**	**-0.01**	**0**	**2**	**-1**
7	**Average**	**0.46**	**0.39**	**0.29**	**0**	**0.4**	**0.1**

Table 29 (Continued)

8	1	0.13	0.49	-0.1	0	0	0
8	2	-0.2	0.04	0.12	0	-1	0
8	3	-0.2	0.03	0.46	0	0	0
8	4	0.58	0.09	0.12	0	1	0
8	5	-0.65	0.09	0.12	0	0	0
8	6	-0.31	0.6	0.68	0	0	0
8	7	-0.54	0.37	-0.66	0	-1	0
8	8	-0.31	0.82	-0.1	0	0	0
8	9	0.13	-0.63	-0.32	0	-1	0
8	10	-0.99	0.15	0.12	0	2	0
8	Average	0.4	0.33	0.28	0	0.6	0
9	**1**	**0.2**	**1.1**	**-0.03**	**0**	**0**	**0**
9	**2**	**0.09**	**0.03**	**-0.03**	**0**	**-1**	**0**
9	**3**	**0.58**	**0.37**	**0.3**	**0**	**-1**	**0**
9	**4**	**0.09**	**-0.41**	**0.07**	**0**	**0**	**0**
9	**5**	**0.42**	**0.93**	**0.19**	**0**	**0**	**0**
9	**6**	**-0.31**	**0.71**	**0.75**	**0**	**-1**	**0**
9	**7**	**-0.36**	**0.03**	**0.07**	**0**	**-1**	**1**
9	**8**	**0.09**	**0.03**	**0.41**	**0**	**0**	**0**
9	**9**	**-0.24**	**0.03**	**0.08**	**-1**	**0**	**0**
9	**10**	**-0.69**	**-0.52**	**0.3**	**0**	**1**	**0**
9	**Average**	**0.31**	**0.42**	**0.22**	**0.1**	**0.5**	**0.1**
10	1	0.54	-0.19	-0.17	0	-1	1
10	2	0.21	0.36	-0.39	0	-1	0
10	3	-0.24	0.25	-0.39	0	0	0
10	4	0.21	0.25	-0.06	0	0	0
10	5	0.32	0.53	0.27	0	0	0
10	6	-0.18	0.14	-0.17	0	-1	0
10	7	-0.46	0.7	-0.62	0	0	0
10	8	-0.35	1.26	0.38	0	0	0
10	9	-0.01	0.47	-0.28	0	0	0
10	10	-0.46	-0.64	-0.06	0	1	0
10	Average	0.3	0.48	0.28	0	0.4	0.1

Table 30: Adjustments for each iteration and transformation parameter for all the half resolution "different times" registration experiments. Code (m.n) : m is the number of patient, n is T1 for T1-T1 experiments and T2 for T1-T2 experiments

Code	Iteration	xy rot (deg)	yz rot (deg)	zx rot (deg)	x trans (voxs)	y trans (voxs)	z trans (voxs)
1.T1	**1-6**	**-1.8**	**0.56**	**-2.13**	**-5**	**-6**	**-1**
1.T1	**7-12**	**-2.36**	**-2.47**	**0**	**-3**	**-3**	**1**
1.T1	**13-18**	**-2.36**	**-0.9**	**-0.67**	**-4**	**-5**	**-1**
1.T1	**19-24**	**-2.36**	**-2.47**	**-0.33**	**-4**	**-3**	**1**
1.T1	**25-30**	**-2.36**	**-0.78**	**-0.33**	**-4**	**-5**	**-1**
1.T1	**31-36**	**-2.36**	**-2.7**	**-0.33**	**-4**	**-3**	**1**
1.T1	**37-42**	**-2.36**	**-0.78**	**-0.33**	**-4**	**-5**	**-1**
1.T1	**43-48**	**-2.36**	**-2.7**	**-0.33**	**-4**	**-3**	**1**
1.T1	**Max Iter**	**-2.36**	**-1.7**	**-0.33**	**-4**	**-4**	**0**
1.T2	**1-6**	**-2.13**	**0.78**	**-2.02**	**-5**	**-5**	**-1**
1.T2	**7-12**	**-2.47**	**-1.68**	**0.67**	**-4**	**-3**	**0**
1.T2	**13-18**	**-1.91**	**-0.56**	**0.22**	**-4**	**-5**	**0**
1.T2	**19-24**	**-1.91**	**-2.81**	**-0.11**	**-4**	**-4**	**0**
1.T2	**25-30**	**-1.91**	**-1.01**	**-0.11**	**-4**	**-4**	**0**
1.T2	**31-36**	**-1.91**	**-1.68**	**-0.11**	**-4**	**-4**	**0**
2.T1	1-6	2.81	-0.9	1.91	5	1	-1
2.T1	7-12	4.61	-0.67	-1.01	1	1	1
2.T1	13-18	5.51	-0.67	1.91	4	1	-1
2.T1	19-24	5.96	-0.67	-0.67	2	1	1
2.T1	25-30	5.96	-0.67	1.91	3	1	-1
2.T1	31-36	5.96	-0.67	0.45	2	1	1
2.T1	37-42	5.96	-0.67	2.13	3	1	-1
2.T1	43-48	5.96	-0.67	0.45	3	1	1
2.T1	Max Iter	5.96	-0.67	1.3	3	1	0
2.T2	1-6	2.25	-0.56	1.91	5	1	-1
2.T2	7-12	4.83	-0.33	-1.01	2	1	0
2.T2	13-18	5.17	-0.33	1.46	3	1	-1
2.T2	19-24	5.96	-0.33	0.67	3	1	-1
2.T2	25-30	5.96	-0.33	1.12	2	1	-1
3.T1	**1-6**	**-1.01**	**-1.01**	**-0.22**	**-1**	**0**	**1**
3.T1	**7-12**	**-2.02**	**-1.8**	**-0.22**	**0**	**0**	**0**
3.T1	**13-18**	**-2.58**	**-1.57**	**-0.22**	**-1**	**0**	**1**
3.T1	**19-24**	**-2.92**	**-1.57**	**-0.22**	**-1**	**0**	**0**
3.T2	**1-6**	**-1.35**	**-0.78**	**-0.11**	**-1**	**-1**	**1**

Table 30 (Continued)

3.T2	**7-12**	**-2.02**	**-2.02**	**-0.22**	**-1**	**-1**	**1**
3.T2	**13-18**	**-2.58**	**-1.91**	**-0.22**	**-1**	**-1**	**1**
4.T1	1-6	-1.46	1.01	-1.35	-1	-2	-1
4.T1	7-12	-2.02	-1.01	0	-1	-1	0
4.T1	13-18	-1.91	0.33	-0.11	-1	-2	-1
4.T1	19-24	-1.91	-0.44	-0.22	-1	0	0
4.T1	25-30	-1.91	0.56	-0.22	-1	-2	0
4.T1	31-36	-1.91	-0.33	-0.22	-1	-1	0
4.T1	37-42	-1.91	-0.33	-0.22	-1	-2	0
4.T2	1-6	-1.57	1.01	-1.46	-1	-2	-1
4.T2	7-12	-2.13	-1.12	0	-1	-1	0
4.T2	13-18	-2.02	0.45	-0.22	-1	-1	-1
4.T2	19-24	-2.02	0.45	-0.33	-1	-1	0
4.T2	25-30	-2.02	0.45	-0.33	-1	-1	0
5.T1	**1-6**	**-3.15**	**0.22**	**-1.23**	**-2**	**-1**	**-1**
5.T1	**7-12**	**-4.5**	**-1.01**	**1.01**	**-1**	**0**	**0**
5.T1	**13-18**	**-4.5**	**0.56**	**0**	**-2**	**-1**	**-1**
5.T1	**19-24**	**-4.61**	**-0.56**	**1.01**	**-2**	**0**	**-1**
5.T1	**25-30**	**-4.61**	**0.33**	**1.12**	**-2**	**0**	**-1**
5.T1	**31-36**	**-4.61**	**0.33**	**1.12**	**-2**	**0**	**-1**
5.T2	**1-6**	**-3.03**	**0.78**	**-1.01**	**-2**	**-2**	**-1**
5.T2	**7-12**	**-4.5**	**-1.46**	**0.9**	**-1**	**-1**	**-1**
5.T2	**13-18**	**-4.27**	**0.22**	**0.33**	**-2**	**-1**	**0**
5.T2	**19-24**	**-4.38**	**0**	**1.46**	**-2**	**-1**	**0**
5.T2	**25-30**	**-4.38**	**0**	**1.23**	**-2**	**-1**	**0**
6.T1	1-6	-1.57	-0.56	-2.58	-17	-3	-4
6.T1	7-12	0.78	-0.67	0.22	-14	-1	0
6.T1	13-18	1.46	-0.67	-0.22	-16	-4	-3
6.T1	19-24	2.02	-0.67	0	-14	-1	-1
6.T1	25-30	2.02	-0.67	0	-16	-4	-2
6.T1	31-36	2.02	-0.67	0	-14	-2	-1
6.T1	37-42	2.02	-0.67	0	-16	-3	-2
6.T1	43-48	2.02	-0.67	0	-14	-2	-1
6.T1	Max Iter	2.02	-0.67	0	-15	-2	-1
6.T2	1-6	-1.46	-0.67	-2.58	-17	-4	-4
6.T2	7-12	0.56	-0.78	-1.68	-13	-1	-1
6.T2	13-18	0.45	-0.78	-1.57	-16	-4	-3
6.T2	19-24	1.46	-0.78	-1.57	-14	-2	-1
6.T2	25-30	1.79	-0.78	-1.57	-15	-4	-3
6.T2	31-36	1.79	-0.78	-1.57	-14	-2	-1

Table 30 (Continued)

6.T2	37-42	1.79	-0.78	-1.57	-15	-4	-3
6.T2	43-48	1.79	-0.78	-1.57	-14	-2	-1
6.T2	Max Iter	1.79	-0.78	-1.57	-14	-3	-2
7.T1	**1-6**	**-2.58**	**-0.45**	**-1.57**	**-5**	**1**	**-1**
7.T1	**7-12**	**-6.52**	**0.45**	**0.9**	**-2**	**2**	**0**
7.T1	**13-18**	**-9.33**	**0.45**	**-1.01**	**-3**	**0**	**-1**
7.T1	**19-24**	**-9.67**	**0.45**	**-0.78**	**-3**	**3**	**-1**
7.T1	**25-30**	**-10.01**	**0.45**	**-0.45**	**-2**	**0**	**-1**
7.T1	**31-36**	**-10.01**	**0.45**	**-0.45**	**-2**	**3**	**-1**
7.T1	**37-42**	**-10.01**	**0.45**	**-0.45**	**-2**	**0**	**-1**
7.T1	**43-48**	**-10.01**	**0.45**	**-0.45**	**-2**	**3**	**-1**
7.T1	**Max Iter**	**-10.01**	**0.45**	**-0.45**	**-2**	**2**	**-1**
7.T2	**1-6**	**-2.13**	**-0.22**	**-1.57**	**-5**	**0**	**-1**
7.T2	**7-12**	**-6.41**	**0.45**	**0.67**	**-2**	**2**	**0**
7.T2	**13-18**	**-9.11**	**0.45**	**-0.9**	**-4**	**-1**	**-1**
7.T2	**19-24**	**-9.78**	**0.45**	**-0.45**	**-3**	**3**	**-1**
7.T2	**25-30**	**-10.23**	**0.45**	**-0.78**	**-3**	**0**	**-1**
7.T2	**31-36**	**-10.23**	**0.45**	**-0.78**	**-3**	**2**	**-1**
7.T2	**37-42**	**-10.23**	**0.45**	**-0.78**	**-3**	**0**	**-1**
7.T2	**43-48**	**-10.23**	**0.45**	**-0.78**	**-3**	**2**	**-1**
7.T2	**Max Iter**	**-10.23**	**0.45**	**-0.78**	**-3**	**1**	**-1**
8.T1	1-6	-0.67	-2.13	0.78	5	8	1
8.T1	7-12	-3.37	-1.23	-1.57	4	8	0
8.T1	13-18	-5.06	-1.68	0.11	4	8	0
8.T1	19-24	-5.73	-1.68	0	5	8	0
8.T2	1-6	-1.01	-2.25	0.9	5	8	1
8.T2	7-12	-3.6	-0.78	-1.68	3	8	0
8.T2	13-18	-5.62	-1.23	1.01	5	8	0
8.T2	19-24	-5.85	-1.12	-1.35	4	8	0
8.T2	25-30	-5.96	-1.12	0.11	4	8	0
8.T2	31-36	-5.96	-1.12	-0.22	4	8	0
9.T1	**1-6**	**0.56**	**0.56**	**-0.78**	**-1**	**0**	**-1**
9.T1	**7-12**	**0.45**	**0.11**	**0.11**	**-1**	**0**	**0**
9.T1	**13-18**	**0.45**	**0.11**	**0.11**	**-1**	**0**	**-1**
9.T1	**19-24**	**0.45**	**0.11**	**0.11**	**-1**	**0**	**0**
9.T2	**1-6**	**0.56**	**1.12**	**-0.9**	**-1**	**-1**	**-1**
9.T2	**7-12**	**0.33**	**-0.56**	**0.56**	**-1**	**0**	**0**
9.T2	**13-18**	**0.33**	**0.9**	**0.33**	**-1**	**0**	**-1**
9.T2	**19-24**	**0.33**	**0.78**	**0.33**	**-1**	**0**	**0**
9.T2	**25-30**	**0.33**	**1.12**	**0.33**	**-1**	**0**	**0**

Table 30 (Continued)

10.T1	1-6	-2.25	0.11	0.33	1	0	1
10.T1	7-12	-3.71	0.33	0.11	0	-1	1
10.T1	13-18	-4.16	0.33	0.11	0	0	0
10.T1	19-24	-4.61	0.33	0.11	0	0	0
10.T2	1-6	-2.58	0.56	0.22	0	-1	1
10.T2	7-12	-4.05	0.67	0.45	0	-1	0
10.T2	13-18	-4.61	0.67	0.45	0	0	1
10.T2	19-24	-5.51	0.67	0.45	0	0	0

Table 31: Adjustments for each iteration and transformation parameter for all the full resolution "different times" registration experiments. Code (m.n) : m is the number of patient, n is T1 for T1-T1 experiments and T2 for T1-T2 experiments

Code	Iteration	xy rot (deg)	yz rot (deg)	zx rot (deg)	x trans (voxs)	y trans (voxs)	z trans (voxs)
1.T1	**1-6**	**-1.91**	**0.67**	**-2.13**	**-8**	**-8**	**-1**
1.T1	**7-12**	**-1.91**	**-1.68**	**0**	**-8**	**-9**	**1**
1.T1	**13-18**	**-1.91**	**-2.47**	**0**	**-8**	**-9**	**0**
1.T1	**19-24**	**-1.91**	**-2.47**	**-0.11**	**-8**	**-9**	**0**
1.T1	**25-30**	**-1.91**	**-2.47**	**-0.11**	**-8**	**-9**	**0**
1.T2	**1-6**	**-2.58**	**0.9**	**-2.14**	**-8**	**-9**	**-2**
1.T2	**7-12**	**-1.68**	**-1.57**	**-0.22**	**-8**	**-11**	**1**
1.T2	**13-18**	**-1.46**	**-2.7**	**-0.11**	**-8**	**-10**	**0**
1.T2	**19-24**	**-1.46**	**-2.02**	**-0.22**	**-8**	**-11**	**0**
1.T2	**25-30**	**-1.46**	**-2.02**	**-0.22**	**-8**	**-9**	**0**
1.T2	**31-36**	**-1.46**	**-2.02**	**-0.22**	**-8**	**-12**	**0**
1.T2	**37-42**	**-1.46**	**-2.02**	**-0.22**	**-8**	**-8**	**0**
1.T2	**43-48**	**-1.46**	**-2.02**	**-0.22**	**-8**	**-12**	**0**
1.T2	**Max Iter**	**-1.46**	**-2.02**	**-0.22**	**-8**	**-10**	**0**
2.T1	1-6	2.92	-0.9	1.91	7	3	-1
2.T1	7-12	5.73	0	-0.45	4	2	1
2.T1	13-18	5.62	0	1.68	7	2	-1
2.T1	19-24	5.85	0	-0.45	4	3	1
2.T1	25-30	5.85	0	1.57	6	3	-1
2.T1	31-36	5.85	0	0.22	5	3	1
2.T1	37-42	5.85	0	1.8	5	3	-1
2.T1	43-48	5.85	0	1.01	5	3	1
2.T1	Max Iter	5.85	0	1.4	5	3	0
2.T2	1-6	2.25	-0.67	2.02	8	1	-1
2.T2	7-12	6.07	-0.11	-0.78	5	2	1
2.T2	13-18	5.62	-0.11	1.68	6	0	-2
2.T2	19-24	6.07	-0.11	0.67	6	3	1
2.T2	25-30	6.07	-0.11	1.01	5	-1	-1
2.T2	31-36	6.07	-0.11	1.57	5	3	0
2.T2	37-42	6.07	-0.11	1.57	5	-1	-1
2.T2	43-48	6.07	-0.11	1.57	5	3	0
2.T2	Max Iter	6.07	-0.11	1.57	5	1	0
3.T1	**1-6**	**-0.9**	**-0.9**	**-0.33**	**-2**	**1**	**3**
3.T1	**7-12**	**-1.68**	**-1.46**	**-0.11**	**-1**	**0**	**1**

Table 31 (Continued)

3.T1	**13-18**	**-1.68**	**-1.46**	**-0.11**	**-2**	**1**	**2**
3.T1	**19-24**	**-1.68**	**-1.46**	**-0.11**	**-2**	**0**	**1**
3.T1	**25-30**	**-1.68**	**-1.46**	**-0.11**	**-2**	**0**	**2**
3.T1	**31-36**	**-1.68**	**-1.46**	**-0.11**	**-2**	**0**	**1**
3.T2	**1-6**	**-1.23**	**-0.78**	**-0.45**	**-2**	**-2**	**2**
3.T2	**7-12**	**-1.91**	**-1.46**	**-0.22**	**-1**	**-1**	**1**
3.T2	**13-18**	**-2.7**	**-1.46**	**-0.22**	**-2**	**-1**	**2**
3.T2	**19-24**	**-2.7**	**-1.46**	**-0.22**	**-2**	**-1**	**1**
4.T1	1-6	-1.46	0.9	-1.12	-3	-4	-2
4.T1	7-12	-1.23	-0.78	0.45	-1	-1	-2
4.T1	13-18	-1.8	0.9	-0.9	-2	-3	-1
4.T1	19-24	-1.8	-0.45	0	-1	-2	-1
4.T1	25-30	-1.8	0.33	-0.78	-2	-2	-1
4.T2	1-6	-1.68	0.89	-1.46	-2	-4	-2
4.T2	7-12	-1.91	-1.23	0	-2	-1	-1
4.T2	13-18	-2.25	1.01	-0.11	-1	-3	-2
4.T2	19-24	-2.25	-1.01	-1.12	-1	-2	-2
4.T2	25-30	-2.25	0.56	-0.56	-1	-2	-2
4.T2	31-36	-2.25	-0.33	-0.56	-1	-2	-2
5.T1	**1-6**	**-3.15**	**0.22**	**-1.35**	**-4**	**-3**	**-2**
5.T1	**7-12**	**-4.5**	**-1.46**	**0.78**	**-2**	**0**	**-1**
5.T1	**13-18**	**-4.5**	**0.67**	**-0.11**	**-3**	**-2**	**-1**
5.T1	**19-24**	**-4.38**	**-1.35**	**0.33**	**-3**	**-1**	**-2**
5.T1	**25-30**	**-4.38**	**0.11**	**0.33**	**-2**	**-1**	**-2**
5.T1	**31-36**	**-4.38**	**-0.33**	**0.33**	**-2**	**-1**	**-2**
5.T2	**1-6**	**-2.92**	**0.67**	**-1.24**	**-4**	**-4**	**-2**
5.T2	**7-12**	**-4.5**	**-1.46**	**0.9**	**-2**	**-1**	**-1**
5.T2	**13-18**	**-4.27**	**0.78**	**-0.11**	**-3**	**-3**	**-2**
5.T2	**19-24**	**-4.38**	**-1.23**	**0.33**	**-3**	**-2**	**-2**
5.T2	**25-30**	**-4.38**	**0.22**	**0.67**	**-3**	**-2**	**-2**
5.T2	**31-36**	**-4.38**	**-0.56**	**0.67**	**-3**	**-3**	**-2**
6.T1	1-6	-1.68	-0.56	-2.36	-18	-6	-4
6.T1	7-12	-2.67	-0.67	-3.71	-29	-2	-6
6.T1	13-18	1.23	-0.67	-1.57	-30	-6	-3
6.T1	19-24	2.36	-0.67	-0.67	-29	-5	-5
6.T1	25-30	2.92	-0.67	-1.12	-29	-6	-4
6.T1	31-36	2.92	-0.67	-1.12	-29	-6	-4
6.T1	37-42	2.92	-0.67	-1.12	-29	-6	-4
6.T2	1-6	-1.57	-0.33	-2.36	-18	-7	-5
6.T2	7-12	-2.58	0	-4.38	-28	-4	-7

Table 31 (Continued)

6.T2	13-18	1.23	0	-2.25	-30	-7	-4
6.T2	19-24	2.47	0	-0.78	-29	-7	-6
6.T2	25-30	3.03	0	-1.12	-30	-7	-4
6.T2	31-36	2.58	0	-0.67	-30	-7	-6
6.T2	37-42	2.58	0	-0.67	-30	-7	-4
6.T2	43-48	2.58	0	-0.67	-30	-7	-6
6.T2	Max Iter	2.58	0	-0.67	-30	-7	-5
7.T1	**1-6**	**-2.36**	**-0.45**	**-1.46**	**-7**	**2**	**-3**
7.T1	**7-12**	**-7.76**	**0.33**	**-0.45**	**-5**	**4**	**-1**
7.T1	**13-18**	**-9.78**	**0.33**	**-1.01**	**-6**	**1**	**-2**
7.T1	**19-24**	**-9.9**	**0.33**	**-0.56**	**-7**	**4**	**-2**
7.T1	**25-30**	**-10.35**	**0.33**	**-0.56**	**-4**	**3**	**-2**
7.T1	**31-36**	**-10.35**	**0.33**	**-0.56**	**-7**	**1**	**-1**
7.T1	**37-42**	**-10.35**	**0.33**	**-0.56**	**-6**	**4**	**-1**
7.T1	**43-48**	**-10.35**	**0.33**	**-0.56**	**-5**	**2**	**-1**
7.T1	**Max Iter**	**-10.35**	**0.33**	**-0.56**	**-5**	**3**	**-1**
7.T2	**1-6**	**-2.36**	**-0.45**	**-1.46**	**-7**	**2**	**-3**
7.T2	**7-12**	**-7.76**	**0.33**	**-0.45**	**-5**	**4**	**-1**
7.T2	**13-18**	**-9.78**	**0.33**	**-1.01**	**-6**	**1**	**-2**
7.T2	**19-24**	**-9.9**	**0.33**	**-0.56**	**-7**	**4**	**-2**
7.T2	**25-30**	**-10.35**	**0.33**	**-0.56**	**-4**	**3**	**-2**
7.T2	**31-36**	**-10.35**	**0.33**	**-0.56**	**-7**	**1**	**-1**
7.T2	**37-42**	**-10.35**	**0.33**	**-0.56**	**-6**	**4**	**-1**
7.T2	**43-48**	**-10.35**	**0.33**	**-0.56**	**-5**	**2**	**-1**
7.T2	**Max Iter**	**-10.35**	**0.33**	**-0.56**	**-5**	**3**	**-1**
8.T1	1-6	-0.9	-2.02	0.9	8	18	1
8.T1	7-12	-4.27	-1.01	-0.45	9	14	2
8.T1	13-18	-5.06	-2.36	-0.9	8	16	0
8.T1	19-24	-5.06	-1.46	-0.9	9	16	2
8.T1	25-30	-5.06	-1.68	-0.9	8	15	1
8.T1	31-36	-5.06	-1.68	-0.9	8	16	1
8.T1	37-42	-5.06	-1.68	-0.9	8	15	1
8.T2	1-6	-0.45	-2.25	0.9	7	18	1
8.T2	7-12	-4.61	-0.45	0	9	14	1
8.T2	13-18	-5.4	-2.13	0	7	15	1
8.T2	19-24	-5.4	-1.57	0	9	14	1
8.T2	25-30	-5.4	-1.8	0	7	15	1
8.T2	31-36	-5.4	-1.8	0	9	14	1
8.T2	37-42	-5.4	-1.8	0	7	14	1
8.T2	43-48	-5.4	-1.8	0	9	14	1

Table 31 (Continued)

8.T2	Max Iter	-5.4	-1.8	0	8	14	1
9.T1	**1-6**	**0.56**	**0.45**	**-0.78**	**-3**	**0**	**-3**
9.T1	**7-12**	**-0.33**	**0**	**1.68**	**-1**	**1**	**0**
9.T1	**13-18**	**-0.33**	**0**	**-0.11**	**-2**	**1**	**-3**
9.T1	**19-24**	**-0.33**	**0**	**0.56**	**-2**	**1**	**0**
9.T1	**25-30**	**-0.33**	**0**	**0.56**	**-1**	**1**	**-3**
9.T1	**31-36**	**-0.33**	**0**	**0.56**	**-1**	**1**	**0**
9.T1	**37-42**	**-0.33**	**0**	**0.56**	**-1**	**1**	**-3**
9.T1	**43-48**	**-0.33**	**0**	**0.56**	**-1**	**1**	**0**
9.T1	**Max Iter**	**-0.33**	**0**	**0.56**	**-1**	**1**	**-1**
9.T2	**1-6**	**0.67**	**1.01**	**-0.9**	**-2**	**-3**	**-2**
9.T2	**7-12**	**0.22**	**-0.67**	**0.56**	**-2**	**0**	**-1**
9.T2	**13-18**	**0.22**	**1.23**	**0.22**	**-1**	**-3**	**-1**
9.T2	**19-24**	**0.22**	**-0.78**	**0.22**	**-1**	**-1**	**-1**
9.T2	**25-30**	**0.22**	**0.9**	**0.22**	**-1**	**-2**	**-1**
9.T2	**31-36**	**0.22**	**-0.11**	**0.22**	**-1**	**-1**	**-1**
9.T2	**37-42**	**0.22**	**0.45**	**0.22**	**-1**	**-1**	**-1**
9.T2	**43-48**	**0.22**	**0.45**	**0.22**	**-1**	**-1**	**-1**
10.T1	1-6	-2.25	0.22	0.33	1	0	2
10.T1	7-12	-3.71	0.45	0.22	1	-1	1
10.T1	13-18	-4.38	0.45	0.22	0	-1	2
10.T1	19-24	-4.72	0.45	0.22	0	-1	1
10.T1	25-30	-4.72	0.45	0.22	0	-1	2
10.T2	1-6	-2.58	0.56	0.33	1	-1	2
10.T2	7-12	-4.05	0.22	0.22	0	-3	1
10.T2	13-18	-4.5	0.22	0.22	0	-1	1
10.T2	19-24	-4.95	0.22	0.22	0	-2	1
10.T2	25-30	-4.95	0.22	0.22	0	-2	1
10.T2	31-36	-4.95	0.22	0.22	0	-2	1

LIST OF REFERENCES

1) Rusinek H, Tsui WH, Levy AV, Noz ME, de Leon MJ. Principal axes and surface fitting methods for three-dimensional image registration. J Nucl Med 1993;34(11):2019-2024.

2) Alpert NM, Bradshaw JF, Kennedy D, Correia JA. The principal axes transformation - A method for image registration. J Nucl Med 1990;31(10):1717-1722.

3) Slomka PJ, Hurwitz GA, Stephenson J, Cradduck T. Automated alignment and sizing of myocardial stress and rest scans to three-dimensional normal templates using an image registration algorithm. J Nucl Med 1995;36(6):1115-1122.

4) Toga AW, Banerjee PK. Registration revisited. J Neurosci Methods 1993;48(1-2):1-13.

5) Turkington TG, Jaszczak RJ, Pelizzari CA, Harris CC, MacFall JR, Hoffman JM, Coleman RE. Accuracy of registration of PET, SPECT and MR images of a brain phantom. J of Nucl Med 1993;34(9):1587-1594.

6) Turkington TG, Hoffman JM, Jaszczak RJ, MacFall JR, Harris CC, Kilts CD, Pelizzari CA, Coleman RE. Accuracy of surface fit registration for PET and MR brain images using full and incomplete brain surfaces. J Comput Assist Tomogr 1995;19(1):117-124.

7) Pelizzari CA, Chen GT, Spelbring DR, Weichselbaum RR, Chen CT. Accurate three dimensional registration of CT, PET and/or MR images of the brain. J Comput Assist Tomogr 1989;13(1):20-26.

8) Junck L, Moen JG, Hutchins GD, Brown MB, Kuhl DE. Correlation methods for the centering, rotation, and alignment of functional brain images. J Nucl Med 1990;31(7):1220-1226.

9) Woods RP, Cherry SR, Mazziotta JC. Rapid automated algorithm for aligning and reslicing PET images. J Comput Assist Tomogr 1992;16(4):620-633.

10) Woods RP, Mazziotta JC, Cherry SR. MRI-PET registration with automated algorithm. J Comput Assist Tomogr 1993;17(4):536-546.

11) Gerlot-Chiron P, Bizais Y. Definition and evaluation of a surface overlap criterion for medical image registration. Prog Clin Biol Res 1991;363: 429-442.

12) Gerlot-Chiron P, Bizais Y. Registration of multimodality medical images using a region overlap criterion. Computer Vision, Graphics, and Image Processing: Graphical Models and Image Processing 1992;54(5):396-406.

13) Kapouleas I, Alavi A, Alves WM, Gur RE, Weiss DW. Registration of three-dimensional MR and PET images of the human brain without markers. Radiology 1991;181:731-739.

14) Strother SC, Anderson JR, Xu XL, Liow JS, Bonar DC, Rottenberg DA. Quantitative comparisons of image registration techniques based on high-resolution MRI of the brain. J Comput Assist Tomogr 1994;18(6):954-962.

15) Venot A, Lebruchec JF, Roucayrol JC. Anew class of similarity measures for robust image registration. Computer Vision, Graphics, and Image Processing 1984;28:176-184.

16) Herbin M, Venot A, Devaux JY, Walter E, Lebruchec JF, Dubertret L, Roucayrol JC. Automated registration of dissimilar images: Application to medical imagery. Computer Vision, Graphics, and Image Processing 1989;47:77-88.

17) Maurer CR, Fitzpatrick JM. A review of medical image registration. In: Maciunas RJ, ed. Interactive Image-Guided Neurosurgery. Park Ridge, IL: American Association of Neurological Surgeons, 1994;17-44. Neurosurgical Topics.

18) Pelizzari CA, Levin DN, Chen GTY, Chen CT. Image registration based on anatomic surface matching. In: Maciunas RJ, ed. Interactive Image-Guided Neurosurgery. Park Ridge, IL: American Association of Neurological Surgeons 1994;47-62. Neurosurgical Topics.

19) Evans AC, Peters TM, Collins DL, Neelin P, Gabe C. Image registration based on discrete anatomic structures. In: Maciunas RJ, ed. Interactive Image-Guided Neurosur-
gery. Park Ridge, IL: American Association of Neurological Surgeons 1994;63-80. Neurosurgical Topics.

20) Weber DA, Ivanovic M. Correlative image registration. Semin Nucl Med 1994;24(4):311-323.

21) Kall BA, Goerss SJ, Kelly PJ, Stiving SO. Three-dimensional display in the evaluation and performance of neurosurgery without a stereotactic frame: More than a pretty picture? Stereotact Funct Neurosurg 1994;63:69-75.

22) Bezdek JC, Hall LO, Clarke LP. Review of MR image segmentation techniques using pattern recognition. Med Physics 1993;20(4):1033-1048.

23) Hall LO, Bensaid AM, Clarke LP, Velthuizen RP, Silbiger ML, Bezdek JC. A comparison of neural networks and fuzzy clustering techniques in segmenting magnetic resonance images of the brain. IEEE Trans on Neural Networks 1992;2:672-683.

24) Press WH, Teukolsky SA, Vetterling WT, Flannery BP. Numerical recipes in C. The art of scientific computing. 2nd ed. New York: Cambridge University Press, 1992.

25) Gonzalez RC, Woods RE. Digital image processing. Addison-Wesley Publishing Company, 1992.